Development of functional films using compatibilization by emulsion techniques

Jeferson Felipe Rio Vicente

Thesis report submitted to

Escola Superior de Tecnologia e Gestão Instituto Politécnico de Bragança

Master's degree in

Chemical Engineering

Within the scope of the double diploma with

Universidade Tecnológica Federal do Paraná Câmpus Apucarana

Supervisors

Profª. Dra. Filomena Barreiro

Dra. Arantzazu Santamaria Echart

Profª. Dra. Caroline Casagrande Sipoli

Bragança, Portugal

2023

ACKNOWLEDGMENTS

To begin the acknowledgments, I would like to quote the famous friar of Isaac Newton: "If I have seen further, it is by standing on the shoulders of giants". For me, these giants were my mentors Caroline Sipoli, Arantzazu Echart, and Filomena Barreiro, who were available throughout the period of carrying out the work available to teach and guide me. Especially Caroline, who was present long before all this happened; she was much more than a teacher; she was also a great friend I gained. I would also like to thank Tatiana Schreiner, who was willing to teach and assist in various stages of this process.

I also could not forget my family Adilson Vicente, Ana Patricia Rio, Cristiane Oliveira, Rodrigo Oliveira, Jhonata Vicente and Jean Vicente who helped me to keep this dream alive. They were the ones who taught me how to live and face everything that could come ahead. Also, they were the basis for getting here, supporting all my decisions. Also, as a family, not by blood but by coexistence, I would like to thank my Brazilian friends that I gained by participating in all of this; I call them my Brigantine family.

I would also like to thank the UTFPR-AP faculty who guided and prepared me, allowing me to participate in all of this. Finally, I would like to thank CIMO and IPB for providing resources and staff to make this experience even better.

The authors are grateful to the Foundation for Science and Technology (FCT, Portugal) for financial support through national funds FCT/MCTES (PIDDAC) to CIMO (UIDB/00690/2020 and UIDP/00690/2020), and SusTEC (LA/P/0007/2020). To Red Cyted ENVABIO100 121RT0108.

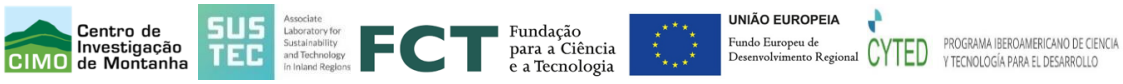

ABSTRACT

Due to the great difficulty in incorporating hydrophobic compounds into hydrophilic matrix films, new strategies for compatibilization have been sought, considering their applications, e.g., food packaging materials. In this context, the present work aims to develop and optimize one of these new strategies, namely by using Pickering emulsions to develop functionalized films from hydrophobic functionalities. For the production of Pickering emulsions and films, biopolymers are commonly used, which can be used to produce particles to act as emulsion stabilizers and as components of the polymeric matrix in the films. In this work, Pickering emulsions were developed based on chitosan (Ch) and gum Arabic (GA), whose ionic bonding, forms a particle complex that stabilizes the emulsion, then added to the film as a carrier of hydrophobic components, which are incorporated in the oil phase. Diverse emulsion parameters were tested, including the oil/water ratio and solid particle concentration, to obtain a stable system to be added to the films (also added with turmeric extract, in a second phase). With the production of the most promising formulation for the emulsion according to an oil ratio of 0.10, and a Ch/GA particle concentration of 4% (w/v) the film-forming solution was prepared an emulsion/aqueous dispersion at a volume ratio of 05/95. It was possible to observe the effects of various factors, such as particle concentration, oil/water ratio, and glycerol content in the emulsions and films. These effects were analyzed concerning the emulsion and the film by analysis of visual inspection, color, morphology, structural and functional analysis by FT-IR, and transparency by UV-vis, among others. For the most promising emulsion formulation with the hydrophobic compound turmeric extract compatibilized, a system with spherical droplets with an average diameter of 3.76 ± 0.70 μm was observed. A yellowish material with a transparency of 18.67% was obtained for the films, demonstrating the influence of the plasticizer agent and the emulsion when compared to the base emulsion.

Keywords: Pickering emulsions; turmeric extract; chitosan; gum Arabic; functionalized films.

RESUMO

Devido à grande dificuldade de incorporação de compostos hidrofóbicos em filmes de matriz hidrofílica, novas estratégias de incorporação e compatibilização têm sido estudadas, levando em conta as suas aplicações, como por exemplo material de embalagem alimentar. Neste contexto, o presente trabalho visa desenvolver e otimizar uma destas novas estratégias, nomeadamente utilizar emulsões Pickering carregadas com funcionalidades hidrofóbicas visando o desenvolvimento de filmes funcionalizados. Para a produção de filmes e emulsões Pickerin*g*, são comumente utilizados biopolímeros, que podem ser utilizados para produzir partículas capazes de atuar como estabilizadores na emulsão e como componentes da matriz polimérica de filmes. Neste trabalho, as emulsões Pickering foram desenvolvidas a partir de quitosano (Ch) e goma Arábica (GA), dois polissacarídeos que podem desenvolver interação iónica, formando complexos que conseguem estabilizar a emulsão, que são posteriormente adicionados a um filme para a incorporação de componentes hidrofóbicos. A criação dos filmes baseou-se no desenvolvimento e otimização de uma formulação estável para a emulsão e estudo de variáveis tais como razão óleo/água e concentração de partículas sólidas e incorporação da emulsão carregada com um extrato de cúrcuma (numa segunda fase do trabalho) em filmes. Após produção da formulação mais promissora para emulsão que compreendeu uma fração de óleo de 0.10, uma concentração de partículas de Ch/GA a 4.0% (p/v), foi produzida a solução formadora do filme utilizando uma razão em volume emulsão/dispersão aquosa de 5/95. Foi possível observar os efeitos produzidos pela variação de fatores como a concentração de partículas, razão óleo/água e conteúdo de glicerol nas emulsões e filmes. Esses efeitos foram analisados a partir da caracterização da emulsão e do filme por análise visual, cor, morfologia, análise estrutural e funcional por FTIR e transparência por UV-vis. Para a formulação de emulsão mais promissora com o composto hidrofóbico extrato de cúrcuma compatibilizado, se observou um sistema com gotas esféricas com diâmetro médio de 3.76 ± 0.70 μm. Um material amarelado com transparência de 18,67% foi obtido para os filmes, demonstrando a influência do agente plastificante e da emulsão quando comparada à emulsão base.

Palavras-chave: Emulsões *Pickering*; extrato de cúrcuma; quitosano; goma arábica; filmes funcionalizados.

TABLE OF CONTENTS

INDEX OF FIGURES

INDEX OF TABLES

LIST OF ACRONYMS

ADS	Average droplet size
Ch	Chitosan
CI	Creaming index
DS	Droplet size
FTIR	Fourier transform infrared spectroscopy
GLY	Glycerol
GSE	Grapefruit seed extract
GA	Gum Arabic
kHz	Kilo Hertz
LDM	Laser diffraction measurement
MPa	Mega Pascal
MV	Microscopic visualization
NOO	Neutral olive oil
O/W	Oil in water
OM	Optical microscopy
RPM	Rotations per minute
SAO	Sweet almond oil
TE	Turmeric extract
VOO	Virgin olive oil
A/O	Water in oil

1. MOTIVATION AND OBJECTIVES

The search for biodegradable polymers plays an essential function in the environmental discussion. Thus, developing new materials with environmental interest and applicability becomes increasingly necessary. In this context, the development of functional biobased films can supply both demands, because those materials are biodegradable and can play a key role in their functionalization.

Biobased functional films prepared through Pickering emulsions have characteristics applicable in various fields, such as food, cosmetics, and pharmaceuticals. Besides that, applying Pickering emulsions into the films brings a broader range of features and possibilities, highlighting as the main function a way to incorporate hydrophobic bioactives within a hydrophilic polymer matrix. When functional biobased films are developed using raw materials such as chitosan and gum Arabic, combining the advantages of both polymers in one material is possible. In addition, adding bioactives, namely turmeric bioactive extract, provides additional biological advantages.

Considering this context, this project aims to develop biobased functional films, based on chitosan and gum Arabic, using the Pickering emulsion technique to enable the incorporation of a hydrophobic bioactive compound, the turmeric extract. This strategy can improve the physical properties of the films and increase their antimicrobial and antioxidant properties, which will be evaluated by determining their physical, chemical, and functional properties.

2. BIBLIOGRAPHIC REVIEW

2.1. COLLOIDAL DISPERSIONS

A system with at least two immiscible phases is called dispersion or colloidal dispersion when the size of the dispersed particles is between 1 and 1000 nanometers (1 nm = 10^{-9} m). This system corresponds to a dispersed phase in a continuous medium. Thus, the possibilities of colloidal liquid dispersions are liquid-gas dispersions; liquid-liquid dispersions, and solid-liquid dispersion (Schramm, 2005).

To summarize and identify the possibilities of the types of colloidal dispersions, a summary of this information is presented in **Table 1**.

Table 1 – Colloidal dispersion types**.** Adapted from (Schramm, 2005; Junior & Varanda, 1999).

Disperse phase	**Disperse medium**	**Name**	**Application**
Liquid	Gas	Liquid aerosol	Fog, deodorant
Solid	Gas	Solid aerosol	Smoke, dust
Gas	Liquid	Foam	Soap or fire-fighting foam
Liquid	Liquid	Emulsion	Milk, mayonnaise, butter
Solid	Liquid	Sol, suspension	Paint, toothpaste
Gas	Solid	Solid foam	Styrofoam®, polyurethane
Liquid	Solid	Solid emulsion	Margarine, opal, pearl
Solid	Solid	Solid suspension	Pigmented glass and plastic

In this context, humanity has used emulsion systems since the early ages, such as clay dispersions for manufacturing ceramics and pigments to decorate the walls of caves (Junior & Varanda, 1999). Nowadays, colloidal dispersions are present daily in various products such as food, cosmetics, pharmaceutical, and many other applications (Rodrigues, et al., 2020).

In addition to classifying the state of the components present in the dispersion, it is important to discuss the size and particle area/volume ratio (Shawn, 1975). Junior & Varanda (1999) defined the concept of polydisperse and monodisperse systems, namely if the population of nanoparticles presents heterogeneity in size, they are classified as polydisperse and nanoparticles of uniform size are cataloged as monodisperse systems.

The formation and characteristics of colloidal dispersions are directly linked to the physical and chemical properties of the components in the system. These properties are very important in the preparation and studies of new materials. (Varanda, 1999).

2.2. EMULSIONS

As specified in the previous section 2.1, liquid-liquid dispersions can be called emulsions; defined as the mixture of two immiscible liquids, using materials or techniques that help to increase the miscibility between both. As an example of emulsions, the milk can be described as an emulsion of fats in water (Atkins, et al., 2017). It is possible to understand the importance of emulsions, highlighting their presence in several areas besides food, such as biomedicine, cosmetics, and pharmaceuticals. (Melle, et al., 2005).

One of the main characteristics of emulsions is their large interfacial area, corresponding to the surface area of the dispersed phase droplets. This feature is the most attractive factor related to its various applications (Berton-Carabin & Schroën, 2015). The droplet size favors appearance, texture, palatability, and flavor. (McClements, 2015).

Emulsions can be classified based on the stability between the phases used and the type of phases, such as oil-in-water (O/W) or water-in-oil (W/O) (McClements, 2012). represents the arrangement of a system with oil and water. **Figure 1** shows the possible rearrangement of water in oil in emulsions.

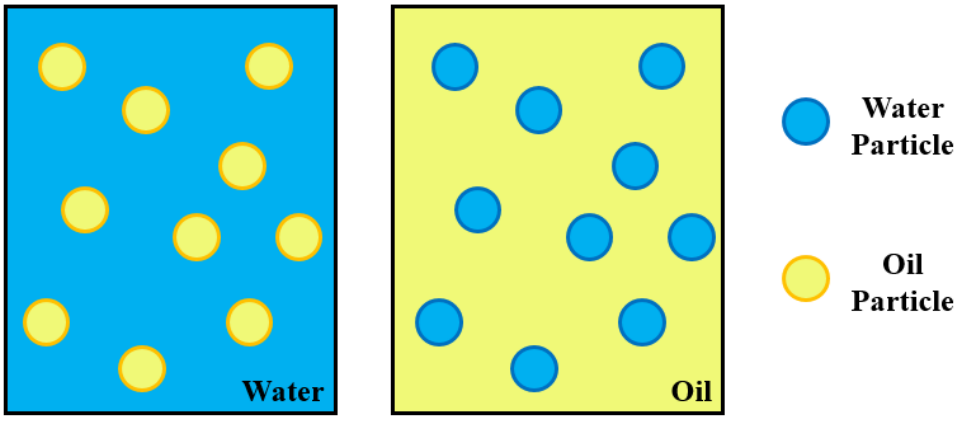

Figure 1 – Emulsions representation **a)** O/W e **b)** W/O. Adapted from (Ghirro, 2019).

O/W or W/O emulsions are thermodynamically unstable because they tend to destabilize over time. (McClements & Jafari, 2018). This destabilization includes physical and chemical phenomena (Zhang, et al., 2020). Different destabilization phenomena are described in **Table 2**, as well as their type (physical or chemical).

Table 2 - Description of the emulsions destabilization phenomena.

Destabilization	Type	Description	References
Sedimentation	Physical	Result of gravitational forces and, consequently, deposition of the dispersed phase.	(Alencar & Ribeiro, 2017)
Flocculation	Physical	It occurs when the Van Der Waals energy of attraction exceeds the energy of repulsion between the micelles, causing the formation of flocs.	(Tadros, 2004)

Destabilization	Type	Description	References
Phase inversion	Physical	An inversion takes place between both phases and the dispersed phase transforms into the continuous phase and vice-versa.	(McClements, 2015)
Ostwald's Ripening	Physical	Given the transfer of matter from smaller to larger droplets by the difference in droplet radio.	(Koroleva & Yurtov, 2021)
Coalescence	Physical	When there is a rupture of the droplets surface causing their union into bigger droplets.	(Silva, 2018)
Creaming	Physical	Effect of gravitational forces that, consequently, suspended the dispersed phase.	(Tadros, 2004)
Oxidation	Chemical	There is a change in the chemical structure of the emulsion by an oxidation phenomenon.	(Hayati, et al., 2005)
Hydrolysis	Chemical	There is a change in the chemical structure of the emulsion by a hydrolysis phenomenon.	(Hayati, et al., 2005)

To minimize the destabilization phenomena, some components or techniques are used. Among the components are surfactants, which are used to improve the stabilization and reduce interfacial energy, preventing the coalescence between emulsion droplets (Manikantan & Squires, 2020). **Table 3** shows some types of surfactants currently used and their characteristics.

Table 3 - Types of surfactants and their description (Salager, 2002).

Surfactant Type	Description
Anionic surfactant	Are dissociated in water in an amphiphilic anion, most often of halogen type.
Nonionic surfactant	Their hydrophilic group is of a nondissociable type, such as alcohol, phenol, ether, ester, or amide.
Cationic surfactant	Are dissociated in water into an amphiphilic cation, which is, in general an alkaline metal (Na^+, K^+) or a quaternary ammonium.
Polymeric surfactant	Association of one or several macromolecular structures exhibiting hydrophilic and lipophilic characters, either as separated blocks or as grafts.

The production of emulsions is directly linked to the type of used stabilizer. For emulsions stabilized with surfactants, usually, low-energy methods are used. To produce these emulsions, magnetic or mechanical homogenizers (low-energy) can be employed. For other types of emulsions, high-energy production methods are used, including ultrasonic energy homogenizers, high-pressure homogenizers, and high-speed homogenizers (Zhou, et al., 2021). Through these methods, the use of solid particles as stabilizers is increasingly studied, known as Pickering emulsions.

2.3. PICKERING EMULSIONS

This emulsion type was firstly studied at the beginning of the 20th century, by Ramsden (Ramsden, 1904) and Pickering (Pickering, 1907), giving the latter the name to this type of emulsions. Unlike conventional emulsions that are stabilized by surfactants, these are, in turn, stabilized by colloidal particles or solid-state particles. (Xia, et al., 2021). In addition, Pickering emulsions have a different stabilization technique, provide better stability, and lower toxicity (Ortiz, et al., 2020). In Pickering emulsions, particles are adsorbed at the oil-water interface, forming a physical barrier that blocks interfacial interactions and contact between the droplets. (Xia, et al., 2021). The formation of this type of emulsion is directly linked to the energy involved in the droplet's formation process and the particles participating in the system. (Low, et al., 2020). The energy needed to separate the particles from the interface can be calculated from **Equation 1** (Briggs, et al., 2018).

$$E = \pi \cdot R^2 \cdot \gamma_{O/W} \cdot (1 \pm cos\theta)^2 \quad (1)$$

where R is the particle radius measured in meters, γ is the interfacial tension measured in $J.m^{-2}$, θ is the contact angle measured in radians, and E is the free energy for the particle to be adsorbed or desorbed at the oil-water interface measured in J.

To determine the formation and stabilization of the emulsion, two factors are fundamental for its stability: the wettability and the dimension of the solid particles. The wettability refers to the contact angle between the oil-particle-water interfaces, a parameter that determines the type of formed emulsion (O/W or W/O). Particles with contact angles in the range $15º < \theta < 90º$ tend to stabilize in O/W emulsions, while particles in the range $90º < \theta < 165º$ are prone to stabilize in W/O emulsions (Ortiz, et al., 2020). This relationship is illustrated in **Figure 2**.

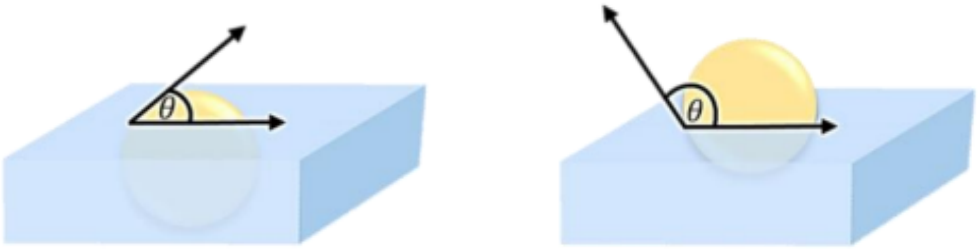

Figure 2 – Contact angle representation to an oil droplet **a)** 15º < θ < 90º (O/W) **b)** 90º < θ < 165º (W/O). Adapted from (Gramatges, 2018).

Regarding the dimension of the Pickering particles, in addition to the stability of the emulsions, it is also responsible for the emulsion droplets size in the continuous medium. (Ortiz, et al., 2020). A relevant point of Pickering particles is that there must be a significant difference between the size of the particles and the formed droplets. (Kaewsaneha, et al., 2013). **Figure 3** shows a schematic representation of a Pickering emulsion (O/W and W/O type).

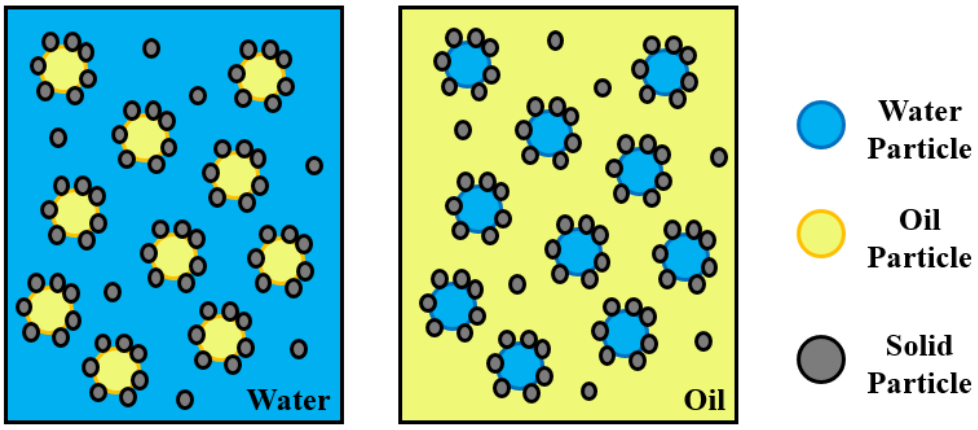

Figure 3 – Schematic representation of a Pickering emulsion type: **a)** O/W e **b)** W/O. Adapted from (Ghirro, 2019).

Since Pickering emulsions have become increasingly relevant systems, the applications of these systems are increasing continuously. **Table 4** summarizes some research carried out in this area, and the associated nature of the used particles.

In this context, Pickering emulsions have many uses and can be prepared from different processes. They can be designed from different single and conjugated materials. In particular, it is possible to cite the use of polysaccharides such as chitosan and gum Arabic.

Table 4 - Particles applied in Pickering emulsions and their description.

Particle type	Application	References
Chitosan-gum Arabic	O/W Pickering emulsions based in polysaccharide particles and free of surfactants for cosmetics application.	(Sharkawy, et al., 2019)
Starch	Starch-based Pickering emulsions for food applications	(Zhu, 2019)
Nanocellulose	Preparation of O/W emulsions for application in drug delivery, food, and composite materials.	(Fujisawa, et al., 2017)
Carboxymethyl cellulose (CMC)	Preparation of O/W emulsions for oil recovery	(Kumar, et al., 2017)
Food-grade gelatin nanoparticles (GNPs)	Application to stabilize Pickering emulsions for food industry applications.	(Feng, et al., 2020)
Soy protein isolate-chitosan (SPI-CS) nanoparticles	Investigate the feasibility of fabricating food-grade Pickering emulsions from alternative proteins.	(Yang, et al., 2020)

As previously mentioned, the fields of application of Pickering emulsions are diverse, from the application as encapsulating agents and/or carriers. This technique can also provide the compatibilization of hydrophilic components in hydrophobic matrices and vice versa, generating dual functional systems (Niro, et al., 2021).

2.4. GUM ARABIC AND CHITOSAN IN PICKERING EMULSIONS

2.4.1 Gum Arabic

Polysaccharides comprise monosaccharide units joined by glycosidic bonds and are a subgroup of carbohydrate molecules (Liu, et al., 2018). In nature, these materials can be found in plants, animals, microorganisms, and algae (Bektas, et al., 2021). Among them, natural gums are highlighted as an attractive option, and their potential is illustrated in **Figure 4**. Natural gums are used due to their low cost, being chemically inert, biocompatible, nontoxic, odorless, and abundant in nature (Mohammadinejad, et al., 2020).

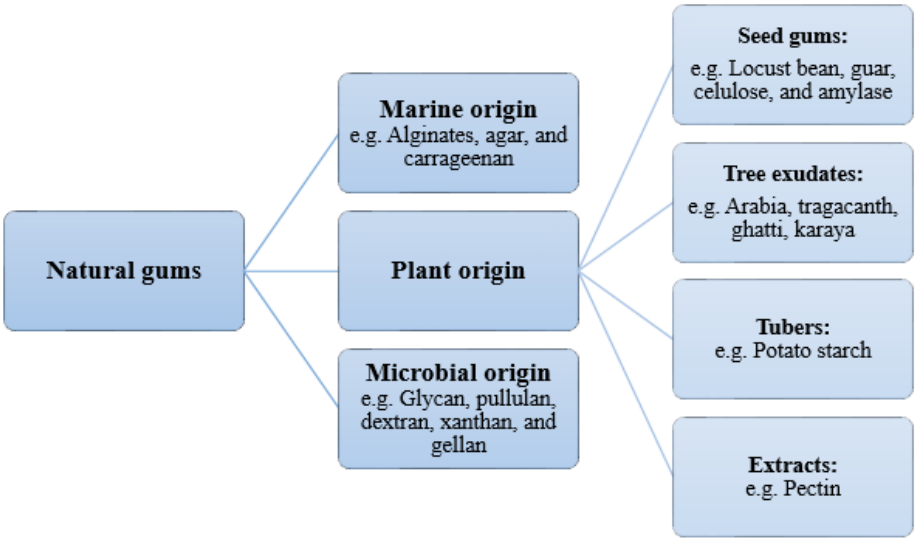

Figure 4 - Natural gums fluxogram. Adapted from (Mohammadinejad, et al., 2020)

An important type of gum is the gum Arabic (GA), obtained from branches and trunks of acacia species, mainly *Acacia senegal* (Jaafar, 2019). That gum is formed by galactosyl, arabinosyl, rhamnosyl, glucuronosyl, and 4-O-methyl-glucuronosyl (Taghavi, et al., 2018). The GA can be used as an emulsifier, and stabilizer in food and cosmetic products containing oil-water interfaces (Dror, et al., 2006); besides that, the GA presents high solubility and low viscosity compared to other polysaccharides (Daoub, et al., 2018). **Figure 5** shows the gum Arabic chemical structure.

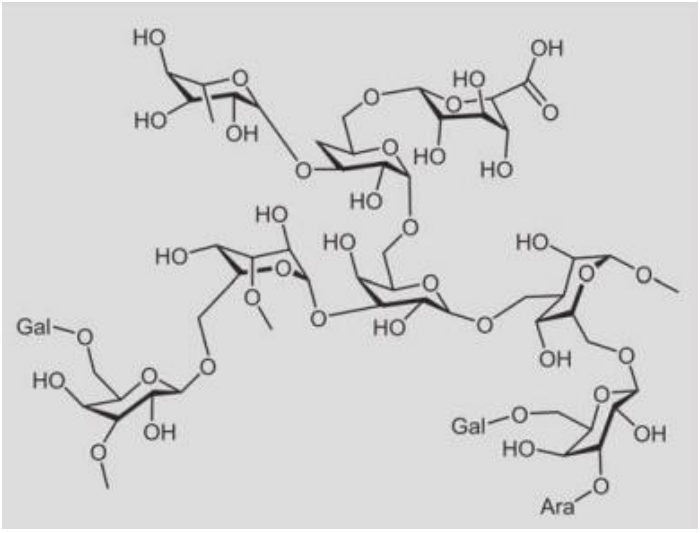

Figure 5 - Gum Arabic chemical structure (Jahandideh, et al., 2021).

Nowadays, the principal use of GA is as an emulsifying agent, whose capacity is attributed to its amphiphilic nature. When the pH is above 2.2 the GA is negatively charged due to the dissociation of the carboxyl groups in its molecular structure. These characteristics favor the utilization of GA in Pickering emulsion, where GA plays the role of electrolyte. Consequently, complexation by electrostatic attraction with other polymers (Isobe, et al., 2020) can be explored to produce particles with potential as Pickering stabilizers.

2.4.2 Chitosan

Many bioactive substances, such as chitosan (Ch), are typically found in marine organisms. Chitosan is a polysaccharide of marine origin produced typically from chitin

extracted from the exoskeletons of crustaceans (Sánchez-Machado, et al., 2019). The growing interest in natural alternatives to synthetic polymers, namely biopolymers, caused the discovery of chitosan (Morin-Crini, et al., 2019).

Chitosan has countless properties, including non-toxicity, biodegradability, biocompatibility, non-antigenic functionality, and low cost. These properties make chitosan a promising compound for applications in pharmaceutical, cosmetics, and food fields (Shariatinia, 2019). Chitosan is a linear polymer chemically composed of D-glucosamine and N-acetylglucosamine monomers linked through β(1-4)glycosidic linkages. As quoted, chitosan is obtained through the deacetylation of chitin (Sahariah & Másson, 2017).

The solid chitosan is a semicrystalline polymer of a white or slightly yellow appearance. The chitosan is obtained when the chitin reaches a degree of deacetylation greater than 50% (Rinaudo, 2006). Chitosan is insoluble in water, alkaline solutions, and organic solvents and soluble in dilute acid solutions below pH 6.3 (Sánchez-Machado, et al., 2019) or at pH values lower than its pKa (<6.5). The amino groups from chitosan become protonated, allowing to interact with negatively charged compounds, such as fatty acids, proteins, and anionic polysaccharides (Sharkawy, et al., 2020). **Figure 6** shows the pH effect, relative to the pKa, in the chitosan structure.

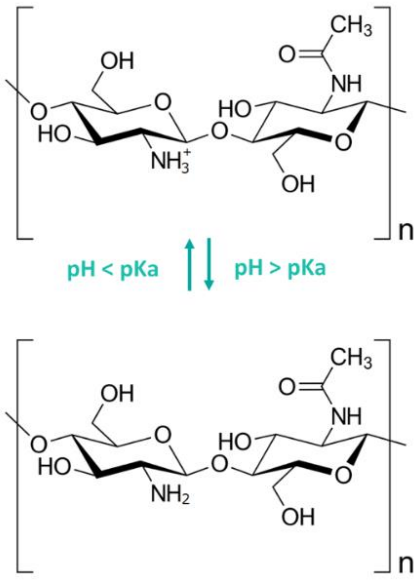

Figure 6 - Forms of chitosan as a function of the pH of the medium (Sharkawy, et al., 2020).

In Pickering emulsions context, chitosan can be used as a stabilizer by complexation with other polymers or through the hydrophobic modification of its structure. An excellent example of the application of chitosan in Pickering emulsions is shown by Han et al (2020), where Ch was used as a hydrophilic compound in the polyelectrolyte complexation with GA, which is an amphiphilic compound. In a solution with pKa < 6.3 the Ch is protonated, gaining positive character. On the other hand, when GA is present in a solution with a pH above 2.2, it is negatively charged. Therefore, using a solution with a pH range of 2.2 to 6.5, it is possible to complex these compounds, forming a nano complex (Han, et al., 2020).

2.5. TURMERIC-BASED EXTRACTS AS FUNCTIONAL INGREDIENTS

The interest in using herbs, teas, medicinal plants, phytomedicines, plant-derived ingredients, and so-called “nutraceuticals” has grown worldwide over the past decades. The chemical, pharmacological, and toxicological research accelerated this interest. This is evidenced by the growth of publications in these areas over three decades, which increased by almost 700% (Heinrich, et al., 2017).

Plants have yielded some of our most essential drugs in the last century. The development of drugs using natural products as “lead” molecules continues, and many plant-derived pure compounds (or natural products) are used in modern drugs (Heinrich, et al., 2017). In this field, it is possible to highlight the use of turmeric, whose scientific name is *Curcuma longa*. Turmeric is a plant, that probably originated in India, and is used for at least 2500 years. Currently, this plant is distributed throughout the tropic and subtropical regions worldwide (Verma, et al., 2018).

Turmeric is a member of the *Zingiberaceae* (ginger) family. The rhizome plant is dried to obtain the turmeric raw material to produce the extracts. This product is known as Curcuma, curcumin, Indian saffron, and yellow ginger (Lauro, 2000). The representation of the initial and final stages of this process is shown in **Figure 7**. The use of this plant is mainly related to the low-cost and high availability. In addition, with the growing search for natural materials, plants are gaining more and more prominence, due to the present bioactive compounds.

Figure 7 - Turmeric rhizome and powder (Eugster, 2014)

This has been evident since antiquity with the use of medicinal herbs. Turmeric is one of the most popular medicinal herbs, with a wide range of pharmacological activities such as antioxidant, anti-protozoal, anti-venom, anti-microbial, anti-malarial, anti-inflammatory, anti-proliferative, anti-angiogenic, anti-tumor, and anti-aging properties (Amalraj, et al., 2017).

All the medicinal properties of turmeric are associated with its chemical composition. It consists of a group of three curcuminoids: curcumin (77%), demetossicurcumin (17%) and bisdemetossicurcumin (3%), as well as volatile oils such as tumerone, atlantone and zingiberone, sugars, proteins, and resins (Hay, et al., 2019). In addition, in the turmeric molecular composition, 326 active compounds were identified (Ahmad, 2020).

Another important point about medicinal plants is the use of extracts, which avoid some disadvantages of using the whole plant. Within these disadvantages, it is possible to mention problems with microbiological agents and/or the requirement for a significantly high amount of plant material that releases the same active substances. In this way, purified extracts are more convenient and safer (Vollhardt, 2000).

Extracts can be classified according to their consistency and the solvent system used in the extraction. The extracts can be found in liquid or concentrated form, being classified between fluid, soft (water percentage between 20% to 25%), or solid extracts (water percentage between 2% to 5%) (Ruivo, 2012). Another important point about the classification is the extract mode.

The extraction mode involves the type of raw material, the solvent, and the method. These three points are directly related to the solubility, stability, bioavailability, pharmacokinetics, pharmacological activity, and toxicity of the extract (Thornfeldt, 2005). Besides that, the extraction method includes the preparation of the raw material

(drying, grinding, homogenization, and or maceration with a solvent) and the extraction stage (macerations, percolation/leaching, infusion, sublimation, distillation, expression) (Ruivo, 2012).

Turmeric extract (TE) can be found in many publications related to evaluating its characteristics, and many others associated with its application. For example, the research of Lira and co-workers (Lira, et al., 2021) evidenced the dependence of TE applications on its features. The work employed the TE obtained from turmeric powder (commercial) and natural turmeric rhizome, including assays about the antioxidant and antimicrobial capacities and the determination of phenolic components; these characteristics show the positive points of using the extract as a possible antioxidant, and antimicrobial agent as well as an aromatic component.

2.6. BIOBASED FUNCTIONAL FILMS

The use of plastics has been seriously discussed due to the disadvantages of their use. More than 300 million tons of plastic are produced worldwide each year. Much of this plastic is not biodegradable, creating environmental problems derived from the waste increase (Ibrahim, et al., 2021). As a countermeasure to using synthetic polymers, biobased alternatives were developed.

Materials that are biobased, biodegradable, or both can be described as biopolymers or bioplastics. These materials include polysaccharides such as cellulose, starch, chitosan, agar, and proteins, and their degradation is faster than the regular polymers under specific conditions. Their applicability includes the food, agriculture, cosmetic, and pharmaceutical sectors (Jiménez-Saelices, et al., 2020). A large part of the conducted research is focused on the food industry because 40% of all plastic production is used in the packaging industry, and 50% of this part is used in the food industry. Therefore, in addition to the issue of creating biopolymers that represent an advance in the environmental struggle, there is also the development of functional films that can have antioxidant, antimicrobial, and many other characteristics that can be used to protect and preserve food (Roy & Rhim, 2021).

To make biobased polymers, renewable sources (biomass) or a mixture of renewable sources and other materials, such as common plastics, resins, and fibers can be used

(Ibrahim, et al., 2021). In this context, the biobased materials are the flagship in the production of functional films because those materials are composed of a polymeric matrix (e.g., polysaccharides) and other compounds that will add the characteristics to the material according to the objective (Batista, 2004).

The main technique to prepare the biofilms is the wet casting of a biobased aqueous solution followed by drying. The choice of the base material and the additive compounds will be crucial to the film's mechanical and physical characteristics. These materials generally cannot be extruded like the other polymers because they do not have a defined melting point, thus causing degradation (Tharanathan, 2003). Another important technique related to biofilms is their functionalization, particularly by incorporating encapsulated bioactives. The encapsulation consists of coating or entrapping one material within another material or system (Risch, 1995).

From the possibility of using polysaccharides to create biofilms, there is also, connected to this, the possibility of using the Pickering emulsion technique as a strong technique that allows the compatibilization of other types of materials with these films. Pickering emulsions, in turn, enable the formation of emulsions using materials that can generate a polymeric matrix and thus form a film with a hydrophobic component in its composition (Sun, et al., 2020).

In the literature, it is possible to see numerous research using biobased materials to produce functional films. For example, using carboxymethyl cellulose/agar to make halochromic films, adding alizarin and grapefruit seed extract (GSE) (Roy & Rhim, 2021). In this work, the author used the carboxymethyl cellulose/agar, a polymeric matrix, alizarin as the pH-reactive compound, and the GSE as a generator of antibacterial and antioxidant functions. Therefore, much research can be seen in scientific literature, considering the advantages of developing and producing functional materials, directly impacting numerous industrial sectors (Jiménez-Saelices, et al., 2020).

3. METHODOLOGIES FOR PICKERING EMULSIONS AND FILMS

3.1. PICKERING EMULSIONS

Pickering emulsions are prepared using an aqueous (hydrophilic phase), oil (hydrophobic phase), and solid stabilizers. These materials are exposed to a high-energy method to mix the compounds (Fu, et al., 2022). The mixing stage can be performed by high-pressure homogenization, rotor-stator, or ultrasonication (Sharkawy, et al., 2020). **Table 5** resumes the description and characteristics of each method and its advantages and disadvantages.

Table 5 - Description and characteristics of mixture methods.

Technique	Description	Advantages/Disadvantages	References
High-pressure homogenization	Consists of a high-pressure pump and a homogenization nozzle. Pressure applied in Pickering emulsions is in the range from 10 to 100 of MPa.	Advantages: Produce large volume samples; utilization in continuous pressure cycles to the same amount; adjust the droplet size. Disadvantages: Operation costs; minimum volume of sample required; temperature increase during the process; high shear rate.	(Albert, et al., 2019) (Ren, et al., 2020) (Chen, et al., 2020)

Technique	Description	Advantages/Disadvantages	References
Rotor-stator	Rotor with blades and a stator with openings, the rotation usually ranges from 5000 to 30000 rpm. The energy involved in this process is attributed to the impact to the rotor and stator, hitting the fluid against the wall.	Advantages: Decrease the droplets size in the emulsion; low operation cost; low liquid volume is needed, speed process. Disadvantages: Distribution of particles with different shapes; minimum particle size limit; high shear rate; temperature rise during the process	(Kempin, et al., 2020) (Kempin & Drews, 2021) (Albert, et al., 2019)
Ultrasonic	Uses a frequency above 16 kHz, which can interact with substances and be used for emulsification mainly by cavitation and ultrasonic forces	Advantages: Small amount of liquid to preparation the emulsions; the possibility to prepare Pickering emulsions with droplets of nanometer size. Disadvantages: Particles degradation; temperature increase during the process	(Chen, et al., 2020) (Albert, et al., 2019) (Cen, et al., 2021)

3.2. FUNCTIONAL FILMS PREPARATION

To functionalize the films, the Pickering emulsion are homogenized in the film-forming solution before applying the casting method, which consists on putting a solution composed of polymers, solvents, and plasticizers, onto a surface, to evaporate the solvent, resulting in the rearrangement of macromolecules to themselves (Farias, 2016).

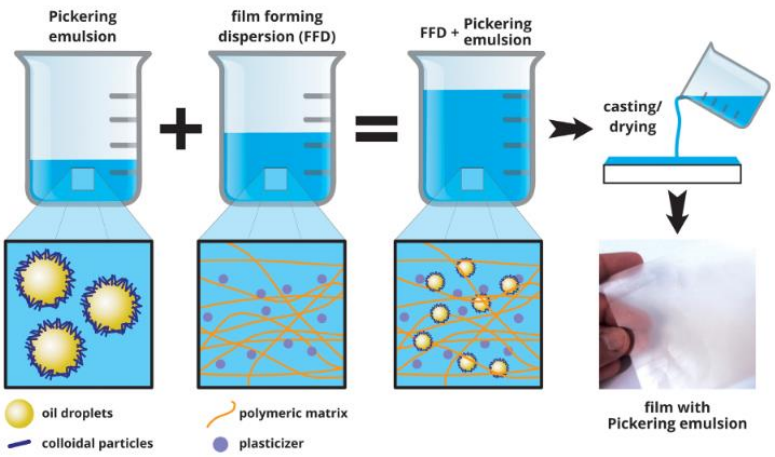

Figure 8 - Diagram of the formation of a film loaded with a Pickering emulsion. Adapted from (Niro, et al., 2021)

Using the casting methodology, the film is formed by solvent evaporation. **Figure 8** represents the process of production a film using Pickering emulsions. Besides the steps described in the **Figure 8**, the addition of the bioactive agent to the Pickering emulsion is necessary in the order it becomes encapsulated in the film forming solution before the casting process (Niro, et al., 2021).

3.3. CHARACTERIZATION

The characterization involves the Pickering emulsions, and, in a second step, the functional films formed. The typically used techniques for both cases are described in the next points.

3.3.1. Pickering emulsions characterization

The size and distribution of the droplets, morphology, and physical stability are typically characterized when Pickering emulsions are produced. The droplet's size and distribution are extremally relevant parameters to determine the stability of the emulsions (Mcclements, 2007). To date, various analytical instruments can be employed to measure

the size and distribution of the droplets in the emulsions. Focusing on droplet size determination, laser diffraction measurement (LDM) and microscopic visualization (MV) are helpful techniques.

Each technique has its advantages and disadvantages. For both methods, it is possible to quantitatively determine the average and droplet size distributions. Regarding disadvantages, for the LDM, the dependence on the emulsion turbidity and the frequent instrument flushing can affect the consistency of the results. In comparison, the MV presents software dependence, the difficulty in the image's visualization and representation only by a small fraction of the sample. Both techniques can be combined to obtain more accurate information (Low, et al., 2020).

Another critical point about Pickering emulsions is their stability, which can be linked to the creaming index (CI) parameter. Hong and co-workers define CI as the parameter that quantifies the phase separation in a Pickering emulsion, which is calculated using the height of the serum layer (aqueous phase) and the total height of the emulsion sample. The serum layer is formed after emulsion destabilization (Hong, et al., 2018).

3.3.2. Functional films characterization

To characterize the films, it is important to evaluate their physicochemical characteristics. These characteristics consider transparency by ultraviolet analysis, color, and Fourier transform infrared spectroscopy (FTIR) techniques (Farias, 2016). These analyses use visual inspection and equipment-assisted results. The transparency and color provide the visual aspect of the films, which corresponds to the primary factor for the consumer in food packaging contexts (Aji, et al., 2018). FTIR analyses will help identify the functional groups present in the films qualitatively, thus providing information for understanding and explaining parameters related to the film.

Another important characterization is the mechanical characteristics of the films, which can be evaluated using a mechanical testing machine to determine the film's tensile properties (Farias, 2016). This technique measures the breaking point, using the applied traction and observed deformation.

Finally, the antibacterial and antioxidant activity are other important features for films aiming at cosmetic, food, or pharmaceutical applications. To the antibacterial activity, it is possible to assess gram-positive and harmful bacteria relevant for the application using the methodology reported by de Campos, et al (2019). The antioxidant activity can be evaluated using the DPPH (2,2-difenil-1-picril-hidrazil) and ABTS (2,2' azino-bis (3-ethylbenzene thiazoline-6-sulfonic acid) assays (Farias, 2016).

4. MATERIALS AND METHODS

4.1. MATERIALS

For this work, Chitosan (Ch) with a deacetylation degree (90% and 85%) from the BioLog Heppe® GmbH (Landsberg, Germany), and spray-dried gum Arabic (GA) from acacia tree obtained from Sigma-Aldrich (St. Louis, MO, USA) were utilized as materials to produce the particles. Other reactives include acetic acid from Honeywell Fluka™ (Lisboa, Portugal), sweet almond oil (SAO) from LabChem (Lisboa, Portugal), virgin olive oil (VOO) purchased from Fagron (Rotterdam, Netherlands), neutral olive oil (NOO) from Vencilab (Serzedo, Portugal), and glycerol obtained from Scharlau (Sentmenat, Barcelona, Spain). The curcumin (derived from Curcuma longa) in powder was supplied by Sigma Aldrich (St. Louis, MO, USA), holding a purity of 65%. Turmeric extract (TE) was provided by UTFPR (Apucarana, Paraná, Brazil) in solid state, produced by hydro-ethanolic extraction of turmeric purchased in local store (Apucarana, Paraná, Brazil). The used distilled water was produced in CIMO (Centro de Investigação da Montanha), Instituto Politécnico de Bragança (Bragança, Portugal).

4.2. METHODS

4.2.1. Ch/GA nanoparticles preparation

The nanoparticles were prepared based on the methodology described in (Sharkawy, et al., 2019). First, the Ch solution was prepared at concentrations of 1.5%, 2.0%, 3.0%, 4.0%, and 5.0% (w/v). For the solutions with the concentration of 1.5%, 2.0%, and 3.0%, 0.1N acetic acid was used, and 0.3N acetic acid was used for the remaining ones. Similarly, GA solution was prepared in water and at the same concentrations. A magnetic stirrer (stirring plate VWR, USA) was used for both solutions' homogenization.

After preparing the solutions, a system composed of a magnetic stirrer (stirring plate VWR, USA) and a peristaltic pump (ISM596B, Ismatec SA, Switzerland) was used. This system was operated to carry out the mixture of the GA solution by dripping it into

the Ch solution at a 1:1 molar ratio under constant agitation at 800 rpm, for approximately 30 minutes. **Figure 9** shows the used system.

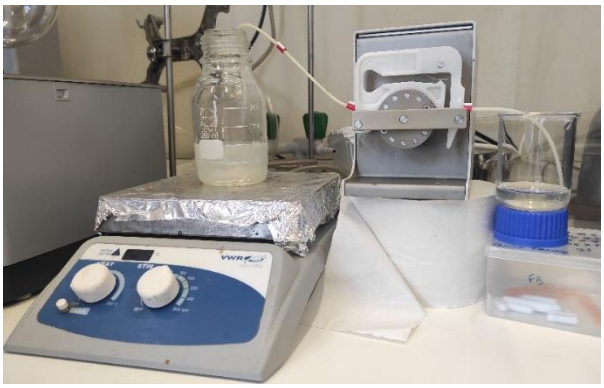

Figure 9 - Ch/GA nanoparticle preparation system.

4.2.2. Pickering emulsions production

Pickering emulsions were prepared based on the methodology described by Sharkawy, et al. (2019). Different oil/water ratios were used (60/40, 50/50, 40/60, 30/70, 27/63, 20/80, 15/85, and 10/90), defined by the oil ratio fraction (ϕ), that is, the oil fraction relative to the total volume. The effect of Ch/GA particle concentration (relative to the aqueous phase, as described in section 4.2.1) was evaluated.

Emulsions were prepared by dropping the oil in the Ch/GA dispersion under stirring (stirring plate VWR, USA) using a peristaltic pump at 3.5 mL/min (ISM596B, Ismatec SA, Switzerland). Then, the mixture was homogenized in an Ultra-Turrax (Unidrive X1000 Homogenizer Drive from CAT Scientific, Staufen, Germany) at 13500 rpm for 7 min. The obtained emulsion was stored at room temperature for analysis.

For the preparation of the loaded emulsions, the needed amount of curcumin or TE (relative to the oil mass) was solubilized into the oil using an ultrasonic bath (SONOREX RX 52, Bandelin, Germany) for 30 min before the emulsion preparation. The same methods for preparing the emulsions mentioned above were used.

Emulsions were coded with the prefix E and, in sequence, the concentration of nanoparticles used, the oil ratio, and finally, the analysis period. To exemplify, the emulsion prepared using nanoparticles at a concentration of 1.5%, with an oil ratio of 0.60, and analyzed right after production was coded as E_1.5%_r0.60_t0.

4.2.3. Films preparation

This film was prepared based on the casting method using a dispersion containing a specific quantity of Ch/GA nanoparticles and the Pickering emulsion at an emulsion/aqueous dispersion volume ratio of 0/100, 75/25, 50/50, 25/75, 15/85, 10/90, and 05/95. Two methodologies were used; in the first, the volume of Ch/GA nanoparticles was collected (according to different emulsion/aqueous dispersion volume ratios), and the Pickering emulsion was added to it, followed by mechanical stirring for 5 min at 900 rpm to obtain the film-forming solution. In the second, the volume of Ch/GA nanoparticles was collected (according to different emulsion/aqueous dispersion volume ratios), and glycerol was added at different concentrations (5%, 10%, 15%, 20%, and 25% relative to the total film mass), followed by mechanical stirring for 5 min at 900 rpm; finally, the Pickering emulsion was added and mechanically stirred for 5 min at 900 rpm to obtain the film-forming solution. The resultant dispersion for both cases was placed in molds (which vary in material and size) and allowed to dry at room temperature for 3 days until the final film was obtained.

Films were coded with the prefix F, followed by the concentration of used nanoparticles, oil ratio, emulsion/plasticizers ratio, glycerol concentration in the film total mass, hydrophobic compound identification (cur – curcumin, TE – turmeric extract) , and hydrophobic compound mass concentration relative to the oil mass. To exemplify, the film prepared using nanoparticles at a concentration of 1.5%, with an oil ratio of 0.60, an emulsion/plasticizers ratio of 10/90, a glycerol mass concentration of 20%, and 0.5% of curcumin was coded as F_1.5%_r0.60_10/90_20%_0.5%cur.

4.2.4. Pickering emulsions characterization

The Pickering emulsions characterization was carried out regarding creaming index, morphology, and colorimetry. The characterization was performed right after Pickering emulsion production (t_0) and 7 days after (t_7).

Creaming index (CI) was calculated by measuring the formed serum layer height in the emulsion (when destabilized). This value is calculated according to **Equation 2**, which expresses the correlation between the height of the serum layer (aqueous phase),

represented by H_S, and the total height of the emulsion sample, represented by H_T (Wang, et al., 2015).

$$CI(\%) = \left(\frac{H_S}{H_T}\right) \times 100 \quad (2)$$

The morphology of the emulsions was analyzed by optical microscopy (OM) using a Nikon Eclipse 50i optical microscope (Kawasaki, Japan) equipped with a Nikon Digital Sight camera, obtaining images of 200x and 400x magnifications. For each emulsion, 50 droplets were measured with the equipment's software, obtaining the average droplet size (ADS) and the standard deviation.

Colorimetry analysis was performed in the emulsions using a portable colorimeter (model CR-400, Konica Monolta Sensing Inc., Japan) equipped with a liquid measuring accessory. The values of the CIELAB scale were determined, namely L*, a*, and b*. The L* value indicates the brightness of the sample; the a* coordinate represents the influence of the green color when negative (-a*) and of the red when positive (+a*); the value of b* manifests the variation of blue when negative (-b*) and yellow when positive (+b*) (De Carli, et al., 2022). **Figure 10** shows the used colorimeter.

Figure 10 - Colorimeter Konica Minalta. (Manual, 2002)

4.2.5. Films characterization

The films were characterized in terms of appearance, and physicochemical characteristics, including the color, the transparency (UV-Vis spectroscopy – UV-Vis), and structural and functional analysis by Fourier transform infrared spectroscopy (FTIR).

The color of the films was analyzed using the colorimeter previously described (model CR-400, Konica Monolta Sensing Inc., Japan; **Figure 10**), using an accessory to evaluate the color of solids.

The transparency of the films was determined using a UV-Vis spectrophotometer (V-730 UV-Visible Spectrophotometer, Tokyo, Japan). The light transmittance (in percentage) was recorded from 200 to 800 nm, referring to the film transparency as the transmittance percentage at 600 nm, corresponding to the visible light and the material thickness in mm (De Carli, et al., 2022). The material transparency can be calculated by the **Equation 3** (Fasihnia, et al., 2020). This equation relates the transmittance (T_{600}) of a material obtained from the transmittance at 600 nm recorded by the equipment and its average thickness (L).

$$Transparency = \frac{\log T_{600}}{L} \quad (3)$$

FTIR analysis was performed using a spectrometer model MB3000 (ABB Inc., Quebec, Canada) equipped with an attenuated total reflection (ATR) accessory. The spectra were recorded between 4000 and 500 cm^{-1} with a resolution of 4 cm^{-1}. This analysis was performed on the base film, the films containing the hydrophobic compound, and used compounds in their production (chitosan, gum Arabic, turmeric extract, curcumin, and sweet almond oil.) The spectra were processed using Horizon MB v.3.4 software (Cologne, Germany).

5. RESULTS AND DISCUSSION

5.1. PRELIMINARY TESTS

Preliminary tests were carried out to set the study's initial point and understand the Pickering emulsions' behavior in the film production context. These tests were developed based on a previous work developed by the group (Sharkawy, et al., 2019), which established the most promising conditions to produce Pickering emulsions using Ch/GA colloidal particles. In this context, to reach the aim of this project, including incorporating the hydrophobic compound and promoting the film-forming capability, the parameters for Pickering emulsions production were adjusted.

Initially, a Pickering emulsion codded as E_1.5%_r0.60 was produced using a Ch/GA nanoparticles dispersion (chitosan with a deacetylation degree of 90%) and virgin olive oil (VOO). The appearance of the emulsion is represented in **Figure 11**.

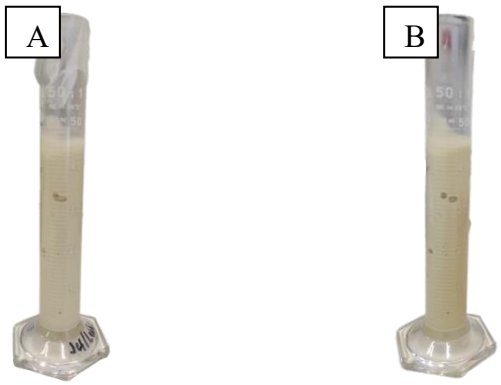

Figure 11 - Pickering emulsion with VOO. (A) E_1.5%_r.0.60_t_0 and (B) E_1.5%_r.0.60_t_7.

The produced emulsion presented a high viscosity and stability. A CI of zero was observed, even at 7 days, showing that the emulsion did not undergo desistabilization within the analyzed period. The comparison between the two times (t_0 and t_7) provided the expected behavior since the reported work showed that the most promising PE formulation resulted using a φ between 0.60 and 0.70.

In **Figure 12** it is possible to see the microscopy of the emulsions at t_0 and t_7. It was possible to visualize that the emulsion droplets had a predominantly spherical shape, but with some elliptic-shape occurrences.

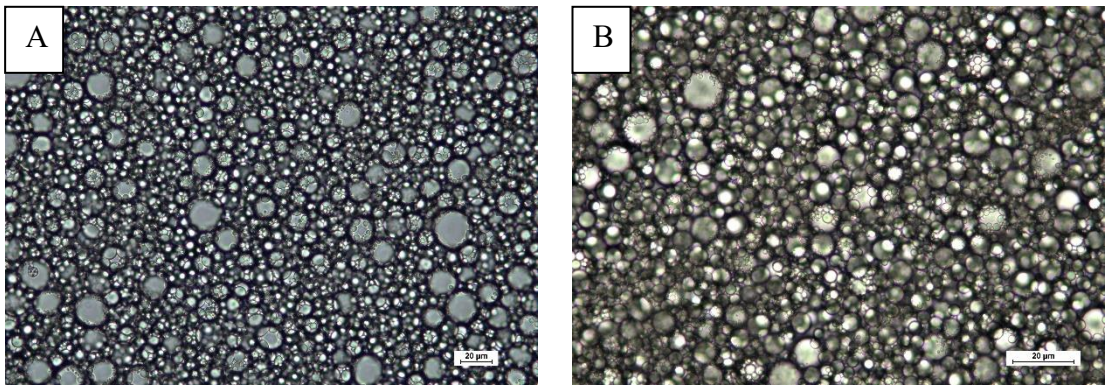

Figure 12 - Pickering emulsion with VOO at 400x magnification; (A) E_1.5%_r.0.60_t_0 and (B) E_1.5%_r.0.60_t_7.

The optical microscopy results were comparable to the ones reported in Sharkawy's work. These results concern the mean droplet diameter and droplet shape. The non-homogeneity in the droplet size distribution could be attributed to the lack of a hydrophobic core, in other words, the formation of free complexes, without the presence of oil inside. In addition, also the lack of a spherical template where the two biopolymers could deposit on (Sharkawy, et al., 2019).

Simultaneously, the film forming capacity of the Pickering emulsion was analyzed. To this aim, an amount of the prepared emulsion was placed in a mold and allowed to dry. The final product is shown in **Figure 13**.

From the obtained product, it was possible to observe an excess of oil and a fragile film, both characteristics are unfavorable to the desired final products. Based on this visualization, it was concluded that the emulsion should have less oil, without affecting its stabilization. Thus, it was fundamental to establish an equilibrium between the emulsion stability and the oil excess in the film. As the first approach, the oil ratio was reduced.

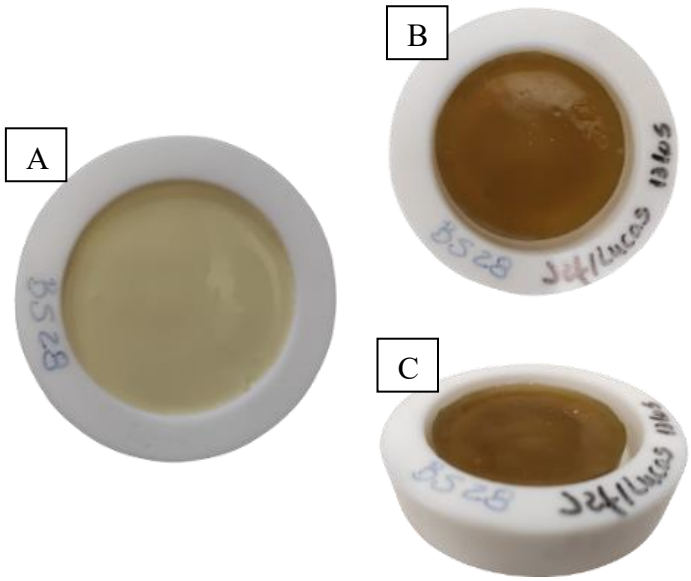

Figure 13 – (A) Film formed with VOO – F_1.5%_r0.60_100/0 before drying; (B) and (C) F_1.5%_r0.60_100/0 after drying.

5.2. PICKERING EMULSIONS AND FILMS COMPOSITION OPTIMIZATION

5.2.1. Base Pickering emulsions and films produced using neutral olive oil

Based on the preliminary tests, the oil ratio was adjusted, and a new emulsion codded E_1.5%_r0.50 and E_1.5%_r0.40 was prepared using neutral olive oil (NOO). **Figure 14** represents the prepared emulsions at t_0 and t_7.

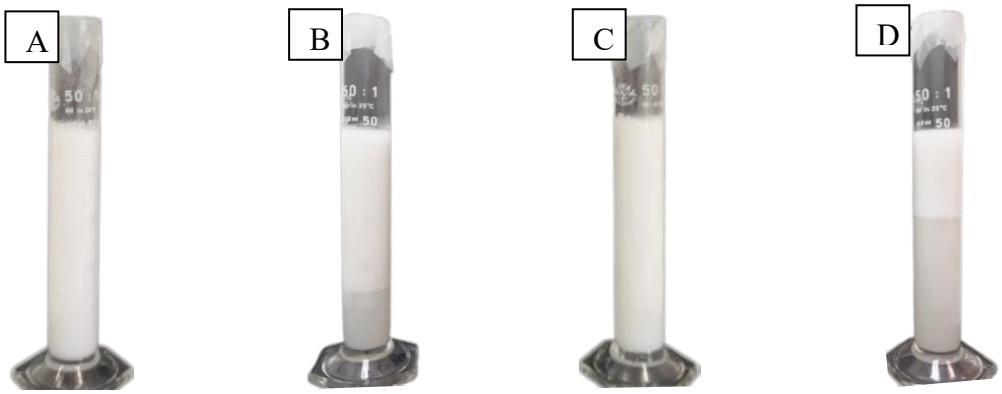

Figure 14 – Pickering emulsions produced. (A) E_1.5%_r0.50_t_0 and (B) E_1.5%_r0.50_ t_7 ; (C) E_1.5%_r0.40_t_0 and (D) E_1.5%_r0.40_t_7.

Comparing the formulations, it was observed that both emulsions presented a serum layer. The emulsion E_1.5%_r0.50 presented a higher stability than the emulsion E_1.5%_r0.40 over time, since the obtained CI values resulted in 28.00% and 62.00%, respectively. These results were expected since the stability of the emulsion is directly linked to the oil ratio; the increase in the oil ratio provides a higher viscosity, which reduces the droplet's mobility preventing their aggregation, reaching the optimal value around $0.70 < \varphi < 0.60$ (Ren, et al., 2022; Sharkawy, et al., 2019).

Figure 15 shows the appearance of the films produced with the emulsions. They showed a similar aspect to the preliminary film, with oil in excess and fragile characteristics. It is important to emphasize that in this case, the emulsion quantity used in the mold was smaller, equal to 15 mL, due to the high film thickness obtained previously.

Figure 15 – Films produced with the emulsions using NOO; (A) F_1.5%_r0.50_100/0 and (B) F_1.5%_r0.40_100/0

The oil excess and the films' fragility impacted the difficulty of handling them. The oil content in the two produced films was calculated and summarized in **Table 6**. It was found that the amount of oil should be reduced in the final film. The weight percentage of each compound in the film confirmed that almost 90% in weight corresponded to the oil. Thereafter, it is important to warranty the increase of Ch/GA proportion in the film composition (after drying).

The Ch/GA mass increase in the final product was attempted by increasing it in the final casting solution. This modification included adding an additional Ch/GA dispersion volume mixed with the emulsion. The addition of the dispersion increased the amount of polysaccharides in the final film, favoring the cohesion of the film matrix.

Table 6 – Composition of the films produced using NOO and Ch/GA dispersion composition.

Φ	Oil (g)	Ch/GA (g)	Composition	
			Oil (%)	Ch/GA (%)
0,50	9,18	0,75	92,45%	7,55%
0,40	7,34	0,90	89,08%	10,92%

5.2.2. Base Pickering emulsions and films produced using sweet almond oil

The formulation was slightly adjusted, considering the needed oil reduction and other related aspects. The first modification implied the NOO replacement by sweet almond oil (SAO), not only due to availability limitations but also because SAO has a higher density (important characteristics able to provide improved stability to the emulsions systems) and does not have accentuated color and smell. The second one involved adding Ch/GA dispersion into the final casting mixture. Finally, due to availability restrictions, the deacetylation degree of the used Ch was changed from 90% to 85%.

Consequently, an emulsion using SAO codded by E_1.5%_r0.50 was produced. The prepared emulsion is shown in **Figure 16**.

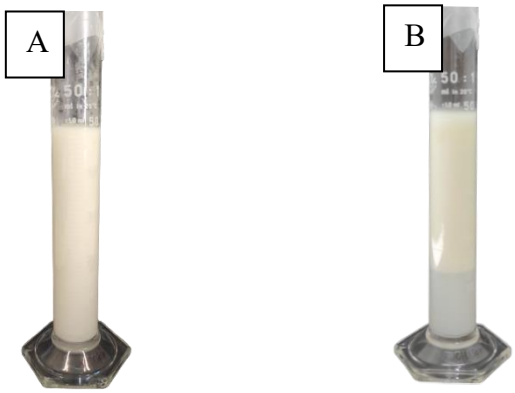

Figure 16 - Emulsion with SAO: (A) E_1.5%_r0.50_t_0 and (B) E_1.5%_r0.50_t_7.

By visual inspection, the emulsion showed instability. It was possible to appreciate the formation of a serum layer 7 days after the production, obtaining a CI of 30,00%. Optical microscopy also confirmed the instability, as shown in **Figure 17**. In **Figure 17-A** (t_0) predominantly spherical shapes and occurrences of some irregular shapes can be

observed. In **Figure 17-B** (t_7) the droplets aggregation was observed, and the regular round shape loss is noticed.

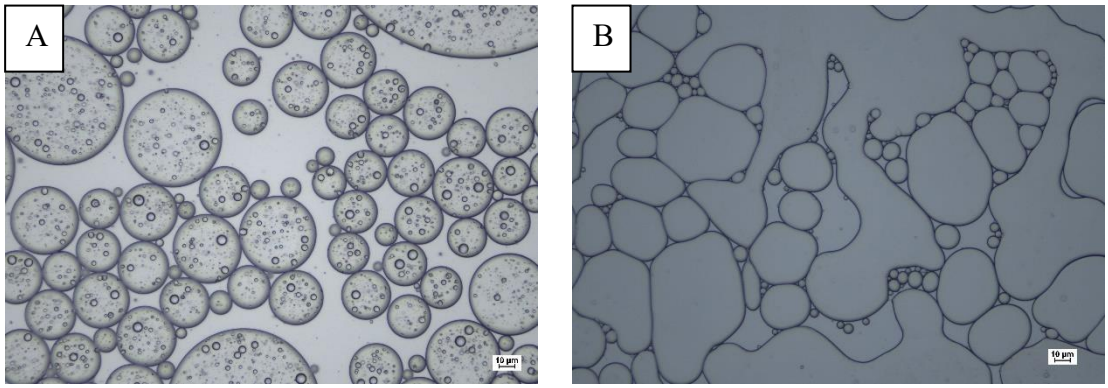

Figure 17 - Pickering emulsion with SAO in 200x magnification; (A) E_1.5%_r0.50_t0 and (B) E_1.5%_r0.50_t7.

The emulsion was utilized to produce films by mixing it with the corresponding Ch/GA dispersion. Three different film systems were prepared, which consisted in diversifying the amount of Ch/GA and emulsion, as summarized in **Table 7**. Using this methodology to produce the films, the Ch/GA mass increase favored the oil amount decrease in the final film.

Table 7 - Films composition (in volume) prepared with the emulsion E_1.5%_r0.50 for 20 mL of film forming solution.

Film	Ch/GA dispersion (mL)	Emulsion (mL)	Mass composition (%)	
			Ch/GA	Oil
F_1.5%_r0.50_75/25	5.00	15.00	3.04	96.96
F_1.5%_r0.50_25/75	15.00	5.00	11.72	88.28
F_1.5%_r0.50_50/50	10.00	10.00	5.39	94.61

The films can be observed in **Figure 18**. **Figure 18-A** represents the system F_1.5%_r0.50_75/25, that contains a higher proportion of the emulsion; **Figure 18-B** rep-

resents the system F_1.5%_r0.50_25/75, which has a higher proportion of Ch/GA nanoparticles dispersion and finally, **Figure 18-C** represents the system F_1.5%_r0.50_50/50, a system with the same proportion of both compounds.

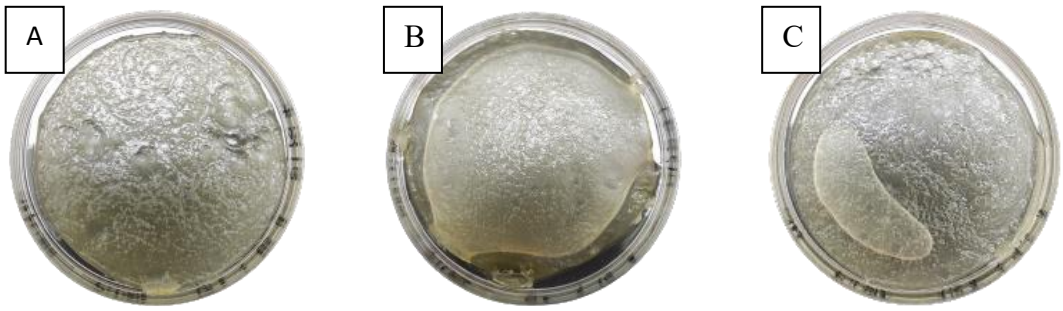

Figure 18 - Films produced using the emulsion E_1.5%_r0.50, according to the (A) F_1.5%_r0.50_75/25, (B) F_1.5%_r0.50_25/75, and (C) F_1.5%_r0.50_50/50.

Comparing the systems, the most promising formulation regarding physical appearance resulted in F_1.5%_r0.50_25/75, which had a higher proportion of Ch/GA dispersion. Nevertheless, an oil excess was also observed in this formulation. The F_1.5%_r0.50_75/25 and F_1.5%_r0.50_50/50 presented oil excess, and fragility problems, similar to the observed in the previous section 5.2.1.

It was possible to see how the high oil quantity influenced the final appearance of the films. Even when decreasing the volume of the used emulsion in the films, it was necessary to propose another approach to solve the oil excess problem and improve the emulsion stability. Under these circumstances, it was decided to increase the concentration of the particles in the aqueous dispersion.

5.2.3. Effect of nanoparticles concentration on the stability of emulsions and film formation

Five formulations with the Ch/GA concentration of 1.5, 2.0, 3.0, and 4.0% w/v were prepared to analyze the impact of the particle's concentration in the emulsions and the films. Concurrently, two additional parameters were modified, including the fixation of the φ at 0.30 and the film formulation in 10% emulsion and 90% dispersion. Using

these conditions, the theoretical oil percentage in the final film would be lower than 65%. Additionally, a formulation with a concentration of 5.0% w/v Ch/GA nanoparticles was also tested, which in turn is presented in **APPENDIX A**. The film formed by this formulation presented deformations, attributed to Ch, which was not completely dissolved due to the high concentration. **Table 8** describes four of the five proposed systems, including the emulsion formulation, CI, and the film's mass composition.

Table 8 – Formulations used to prepare the emulsions and films at a fixed φ of 0.30, associated CI, and the film composition.

Emulsion		**Films**		
Formulation	**CI on t7 (%)**	**Formulation**	**Ch/GA (%)**	**Oil (%)**
E_1.5%_r0.30	62.00	F_1.5%_r0.30_10/90	34,82%	65,18%
E_2.0%_r0.30	49.00	F_2.0%_r0.30_10/90	39,81%	60,19%
E_3.0%_r0.30	2.00	F_3.0%_r0.30_10/90	49,80%	50,20%
E_4.0%_r0.30	10.00	F_4.0%_r0.30_10/90	56,95%	43,05%

Ch/GA and Oil percentages in relation to the film total mass

Figure 19 shows the appearance of the emulsions (t_0 and t_7). The emulsions at t_0 showed to be stable (CI of 0). At t_7 the emulsions E_3.0%_r0.30 and E_4.0%_r0.30 showed higher stability over time than formulations E_1.5%_r0.30 and E_2.0%_r0.30, effect evaluated according to the CI present in **Table 8**.

The increase of the Ch/GA concentration can cover a larger interfacial area that allows for reducing the interaction of the droplets (Mwangi, 2016). This effect reflected the higher stability of formulations E_3.0%_r0.30 and E_4.0%_r0.30. In the case of formulation E_4.0%_r0.30, an additional effect was observed, attributed to chitosan. Considering its low solubility in water, the high solid concentration of chitosan could supersaturate the system, inducing a destabilization phenomenon.

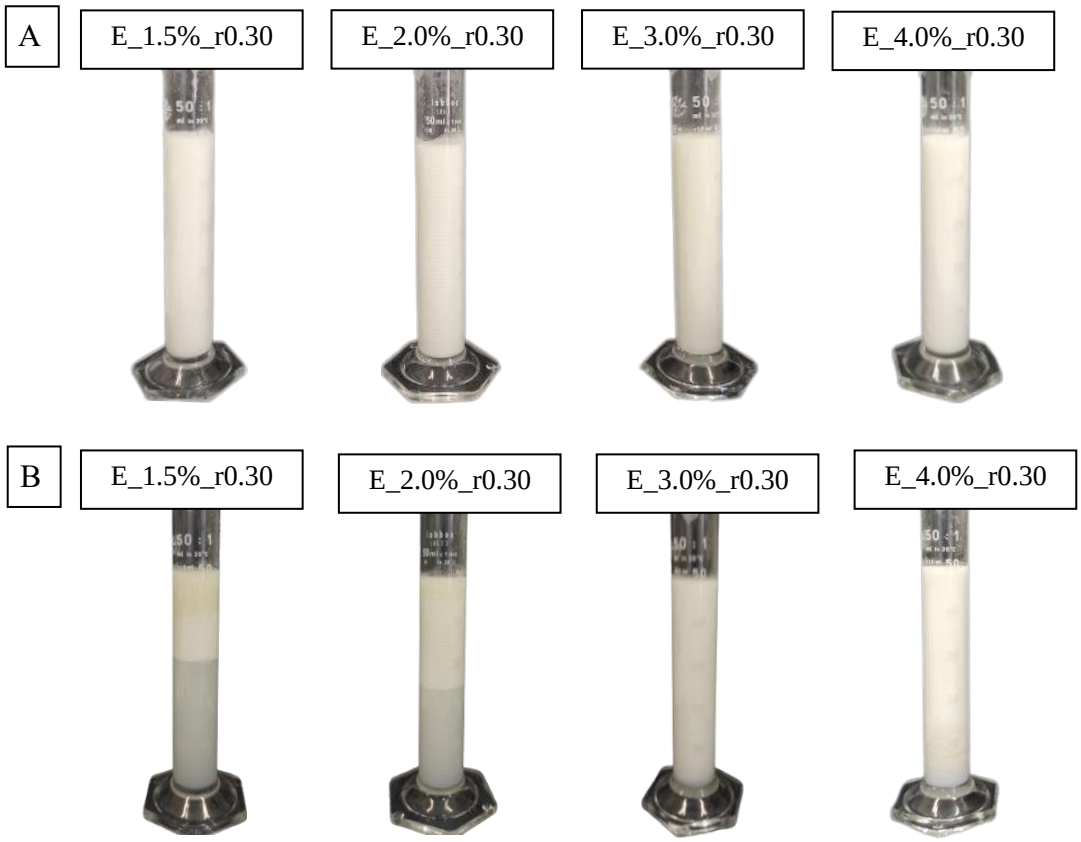

Figure 19 - Emulsions with φ fixed at 0.30 in (w/v) at (A) t_0 and (B) t_7.

Analyzing the optical microscopy results in **Figure 20**, it is possible to see the droplet's deformation and aggregation only for the 1.5% Ch/GA emulsion. The particle size and shape varied with the Ch/GA concentration, being bigger at lower Ch/GA concentrations. This phenomenon can be explained by the increase in the interfacial area covered by the particles in the system.

Observing the obtained films, it was possible to select the most promising formulations, in this case, E_3.0%_r0.30 and E_4.0%_r0.30. The formulations E_1.5%_r0.30 and E_2.0%_r0.30 presented the same problem previously exposed, i.e., oil excess and high fragility. The formulation E_4.0%_r0.30 gave rise to some irregularities in the formed film attributed to the supersaturation of chitosan. The films are shown in **Figure 21**.

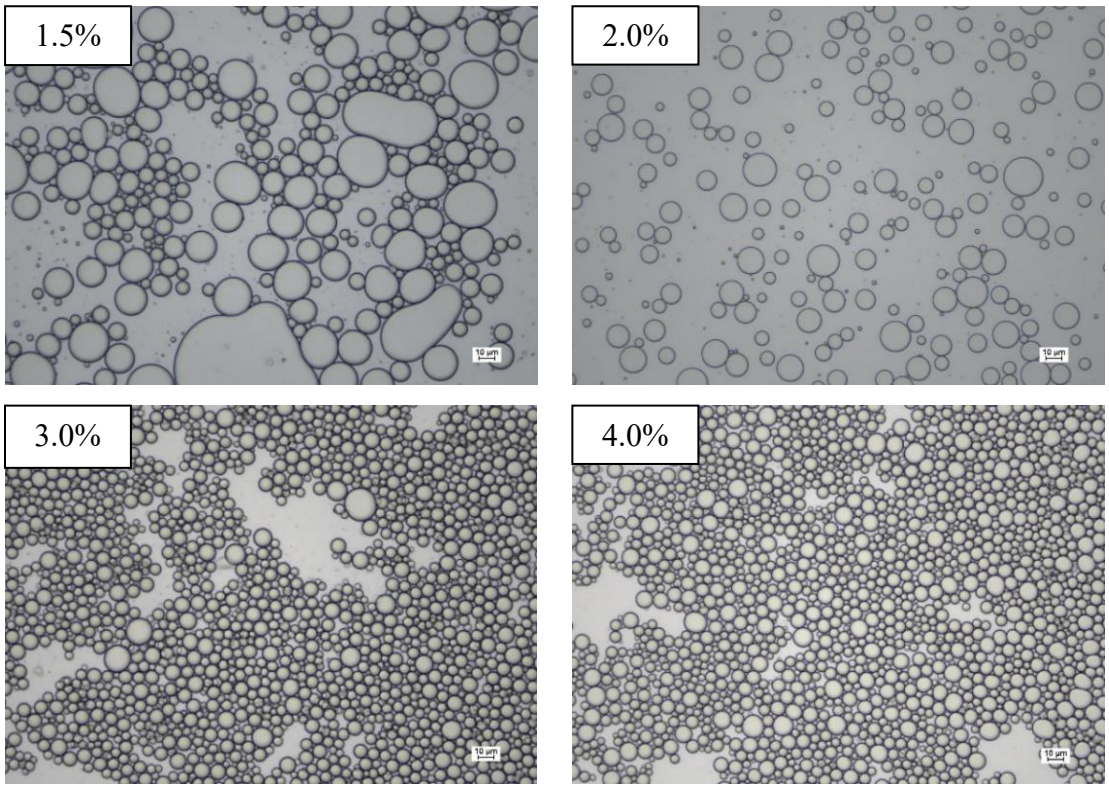

Figure 20 - Optical microscopy at 200x magnifications of emulsion with φ = 0.3 and different concentrations of solids.

Analyzing the results obtained with the different formulations, and the positive aspects mentioned for formulations E_3.0%_r0.30 and E_4.0%_r0.30, it was considered that the optimal formulation for both, the emulsion, and the film, were achieved. The φ of the Pickering emulsion was changed from 0.30 to 0.27 maintaining a Ch/GA at 3.0 and 4.0% (w/v). Particularly, for the Ch/GA at 4.0% (w/v) the acid acetic solution concentration was modified from 0.1 to 0.3N. The increase in the acetic acid concentration favors the solubility of the Ch, attributed to the greater amount of H_3O^+ groups, which interacts with the NH_2 groups present in the chitosan structure (Pardo-Castaño & Bolaños, 2019). In addition, the change was evaluated to provide a favorable range of pH to the Ch and GA complexation.

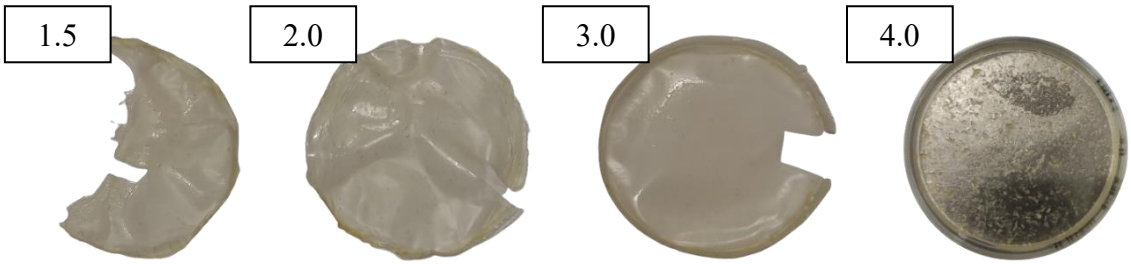

Figure 21 - Films formed using 90% of aqueous dispersion and 10% of the emulsion with φ = 0.3 at their respective dispersion concentrations.

The emulsions and films were prepared following all the proposed changes. The emulsions can be visualized in **Figure 22**, including at t_0 and t_7. These emulsions presented a lower viscosity than the ones of the preliminary tests, due to the lower φ used to produce these emulsions. **Figure 22** shows that the emulsions presented a white coloration and high stability since the calculated CI was zero for both formulations (at t_0 and t_7). Additionally, two tests (production of emulsions E_4.0%_r0.20 and E_5.0%_r0.20, for comparison) were carried out to evaluate the effects of the modifications. These tests are presented in **APPENDIX B**.

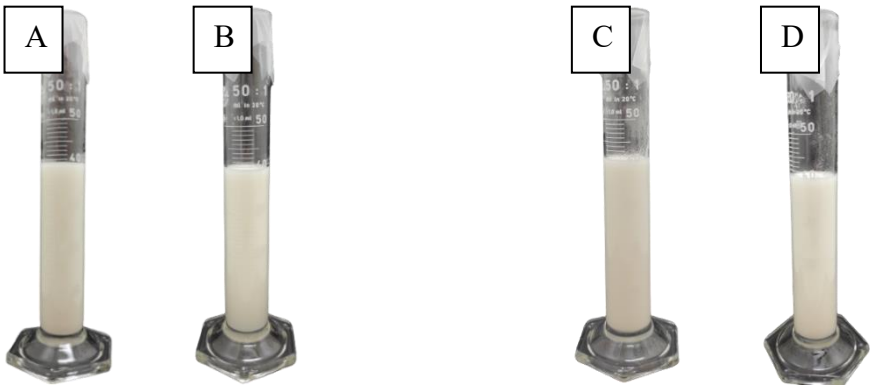

Figure 22 - Emulsions produced using φ = 0.27. (A) E_3.0%_r0.27_ t_0, (B) E_3.0%_r0.27_ t_7, (C) E_4.0%_r0.27_ t_0, (D) E_4.0%_r0.27_ t_7.

Analyzing the microscopic images of the emulsions, **Figure 23** shows a slight increase in the droplet size for both emulsions and a larger spherical shape distribution between t_0 and t_7. Even at the macroscopic scale, it was impossible to see a serum layer formation, microscopically there were some slight signs of coalescence marked by the

increase in the average droplet size (ADS); this difference can also be attributed to deviations in the observed populations.

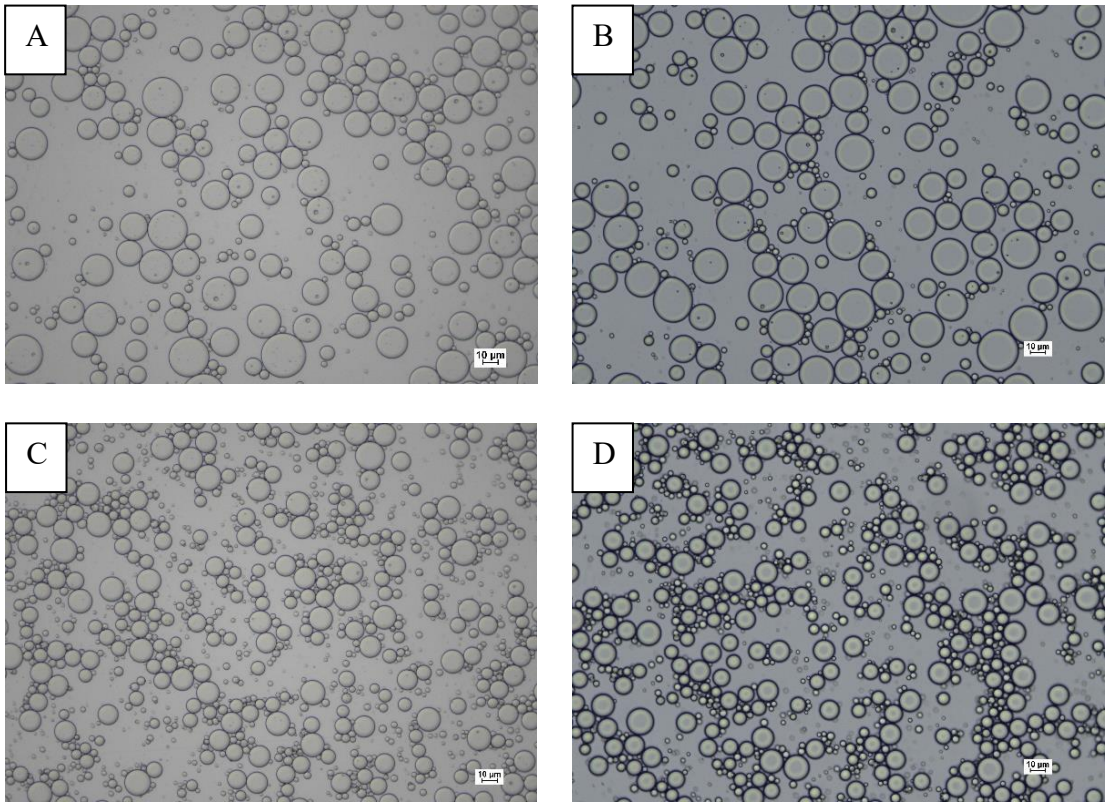

Figure 23 - Emulsions microscopy at 200x magnifications. (A) E_3.0%_r0.27_ t_0, (B) E_3.0%_r0.27_ t_7, (C) E_4.0%_r0.27_ t_0, (D) E_4.0%_r0.27_ t_7.

From the microscopy analysis, it is also possible to confirm the effect of Ch/GA concentration on the droplet size. The ADS of 4.0% (w/v) Ch/GA dispersion provided a lower droplet size value than the ADS of 3.0%. These values are presented in **Table 9**.

Table 9 – Average droplet size of the emulsions at a φ = 0.27.

Emulsion	**t_0**	**t_7**
	ADS (µm)	**ADS (µm)**
E_3.0%_r0.27	12.38 ± 5.48	13.73 ± 6.58
E_4.0%_r0.27	6.54 ± 4.02	7.41 ± 4.06

The films prepared using these formulations showed an improved appearance compared to the previous formulations, as shown in **Figure 24**. In fact, it was favored by using a higher Ch/GA concentration (also in the aqueous dispersion) and the proportion of 10/90 of emulsion and dispersion. Nevertheless, both films showed a high oil amount and fragility. In the final composition, the film using 3.0% (w/v) Ch/GA dispersion contained 47.57% of oil, while the film using 4.0% (w/v) Ch/GA dispersion presented 40.49%. In comparison, the film using 4.0% (w/v) Ch/GA showed a more promising aspect, being selected to adjust the working conditions.

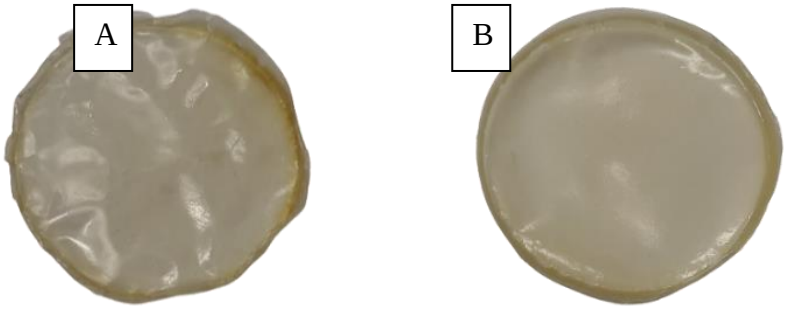

Figure 24 - Films prepared using the emulsion with φ = 0.27 at Ch/GA dispersion with concentration at (A) 3.0% (w/v) and (B) 4.0% (w/v).

The emulsion produced from SAO with Ch/GA dispersion at a concentration of 4.0% (w/v) proved to be efficient in terms of stability when using low oil ratios; therefore, this formulation was established as a base point for the next emulsions and films production.

5.2.4. Pickering emulsions and films production by adding glycerol

Since films produced from the emulsion E_4.0%_r0.27 showed promising results, modifying the emulsion and film formulation even to a lower φ (< 0.27) was proposed. The use of glycerol also reduces the film's fragility, making it more malleable. Systems with φ = 0.2 added with glycerol (GLY) as a plasticizing agent were selected for the next stage. Using plasticizers provides polymer chains with decreased intermolecular forces, increasing the mobility of the polymer network and flexibility (Jha, 2020). To investigate the effects of GLY on the films, it was introduced in proportions relative to the film mass.

An emulsion with φ = 0.2 and Ch/GA dispersion at 4.0% (w/v), codded by E_4.0%_r0.20 was prepared and used to prepare different films. Its stability was verified visually and by optical microscopy. The emulsion appearance is present in **Figure 25**, It was possible to confirm the absence of a serum layer formation, highlighting the emulsion stability and a CI equal to zero, for t_0 and t_7.

Figure 25 – Emulsion (A) E_4.0%_r0.20_t_0 and (B) E_4.0%_r0.20_t_7.

The microscopic analysis, in **Figure 26**, showed that the average droplet size (ADS) increase resulted in slight coalescence at the microscopic scale. Similar ADS values were obtained by comparing with the emulsion using φ = 0.27. The ADS is similar, being possible to observe the lower variation for each sample; the ADS value increased between the two times, namely when using φ = 0.20, it was observed an ADS equal to 6.75 ± 2.60 for t_0 and 7.21 ± 2.67 for t_7. **Figure 26** shows the microscopy analysis that was used for comparison.

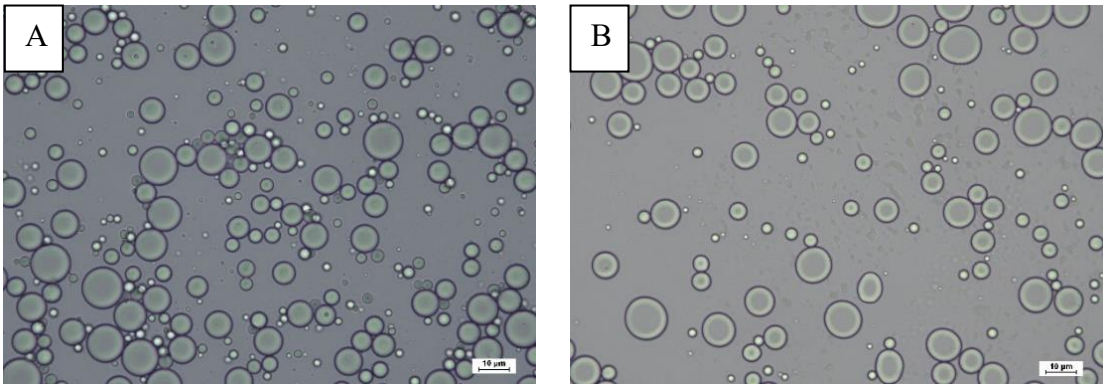

Figure 26 - OM with 400x magnifications of emulsions (A) E_4.0%_r0.20_t_0 and (B) E_4.0%_r0.20_t_7.

The films prepared based on the emulsion E_4.0%_r0.20_t_0 are shown in **Table 10**, as well as their composition and visual description after production. In general, some alterations in the properties of the films were observed with the increase of GLY. The properties of plasticizers can justify this effect; this property concerns the capacity of the plasticizer to interact with the polymer chains extending their distance, weakening the interaction between the components (Teixeira, et al., 2021). In fact, with the Ch and GA interactions weakened, their individual properties are evidenced, in this case, observing a yellowish color of higher intensity characteristic of Ch, observed for the highest concentrations of GLY (Teixeira, et al., 2021).

From the obtained results it was possible to verify the improvement of some visual aspects in the films. Concurrently, the need to reduce the amount of the used oil is still needed. For that, two φ ratios were studied, defined at 0.15, and 0.10. In addition to these tests, a concentration of GLY of 25% (total mass basis) was also used, which was unsatisfactory because the presented film still contained excess oil and had a high malleability, which is a negatively judged factor. The formed film is shown in **APPENDIX C**. From the observations, the best percentage of GLY was determined as 20%.

Table 10 - Appearance and characteristics of films formed with the emulsion E_4.0%_r0.20_t_0.

Film	Composition	Observations
F_4.0%_r0.20_10/90 	Oil – 31.65% Ch/GA – 68.35% GLY – 0%	Brittle, fragile, hard, slightly yellow, and oil excess.
F_4.0%_r0.20_10/90_5% 	Oil – 29.87% Ch/GA – 64.31% GLY – 5.82%	Brittle, fragile, hard, slightly yellow, easier to handle than the F_4.0%_r0.20_10/90, and oil excess.

Film	Composition	Observations
F_4.0%_r0.20_10/90_10% 	Oil – 28.08% Ch/GA – 60.26% GLY – 11.62%	Less Brittle, less fragile, less hard, yellowish, easier to handle than the F_4.0%_r0.20_10/90_5%, and oil excess.
F_4.0%_r0.20_10/90_15% 	Oil – 26.38% Ch/GA – 56.41% GLY – 17.21%	More yellowish than the 3, stronger shades of yellow easier to handle than the F_4.0%_r0.20_10/90_10%, and oil excess.
F_4.0%_r0.20_10/90_20% 	Oil – 24.34% Ch/GA – 51.79% GLY – 23.87%	Strongly yellowish, easier to handle than F_4.0%_r0.20_10/90_15%, and oil excess.

Two new emulsions were prepared according to the quoted φ, maintaining the Ch/GA dispersion concentration at 4.0 % (w/v), as can be observed in **Figure 27** for t_0 and t_7.

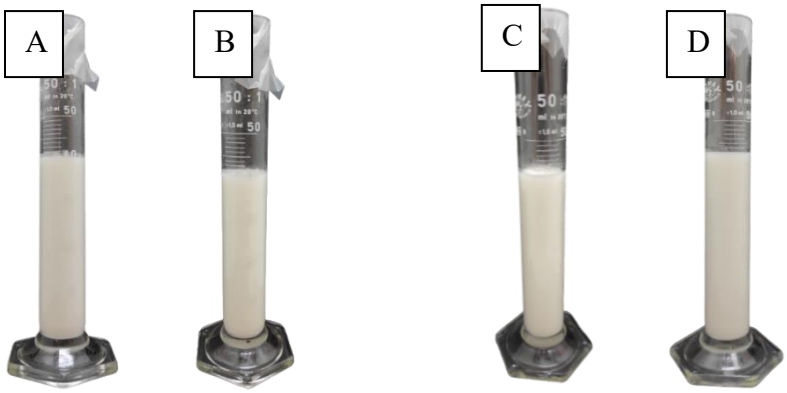

Figure 27 - Emulsions (A) E_4.0%_r0.15_t_0, (B) E_4.0%_r0.15_t_7, (C) E_4.0%_r0.10_t_0, and (D) E_4.0%_r0.10_t_7.

The optical microscopy analysis of the emulsions is shown in **Figure 28** and the ADS determined from each image are summarized in **Table 11**. Both emulsions presented a CI equal to zero, and some differences were observed through optical microscopy between the two emulsions. The emulsion with higher φ presented a higher ADS. This is due to the decrease in the total amount of nanoparticles available to be absorbed at the oil/water interface (Atarian, et al., 2019).

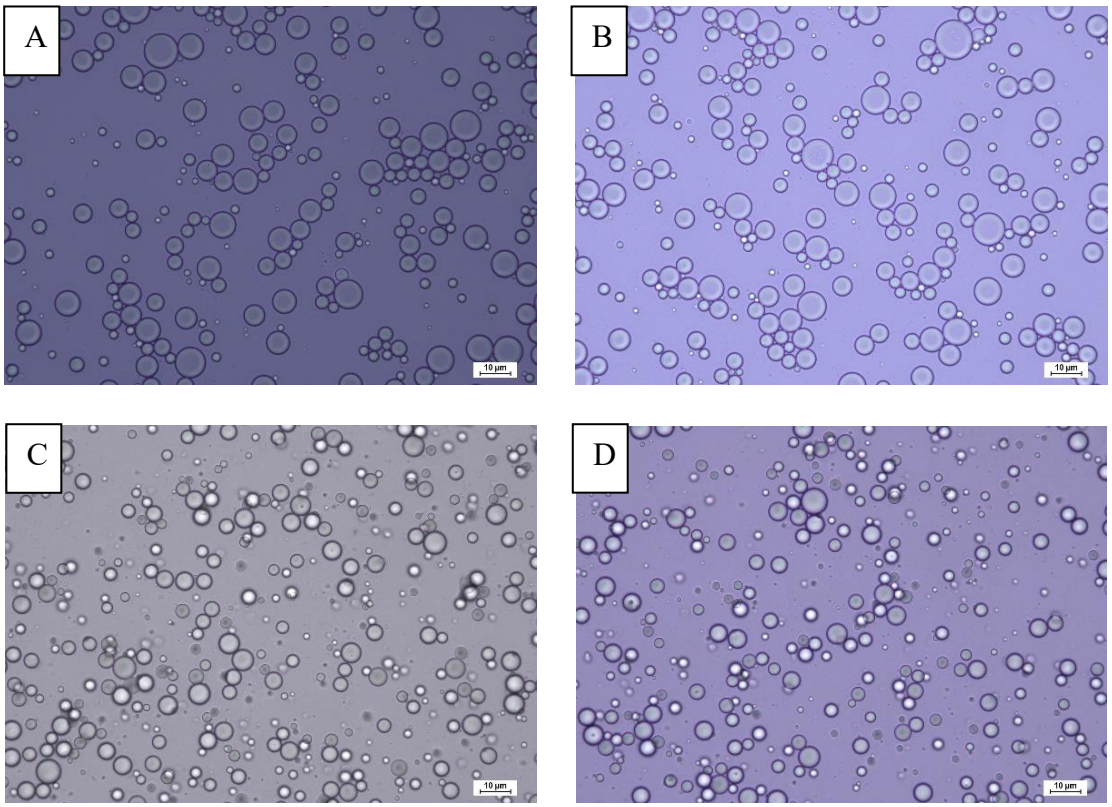

Figure 28 - Microscopy with 400x magnifications of the emulsions (A) E_4.0%_r0.15_t_0, (B) E_4.0%_r0.15_t_7, (C) E_4.0%_r0.10_t_0, and (D) E_4.0%_r0.10_t_7.

Table 11 - ADS of the emulsions.

Emulsion	**ADS (µm)**	
	t_0	**t_7**
E_4.0%_r0.10	3.56 ± 1.36	4.94 ± 1.06
E_4.0%_r0.15	4.99 ± 1.84	5.58 ± 1.73

From **Table 11** it is possible to observe a slight coalescence effect at the microscopic order, showing a tendency of the ADS values to increase over time. Comparing the emulsions E_4.0%_r0.15 and E_4.0%_r.010, the oil ratio effect can be visualized in the emulsion morphology, looking at the obtained ADS.

Films were prepared using the emulsions previously described. In addition, an emulsion/dispersion ratio of 10/90 was used plus 20% glycerol in 20% relative to the theoretical final mass of the film. Their appearance is shown in **Figure 29**. The film formed using the ratio φ = 0.15 showed satisfactory malleability and appearance. However, when handling the film, it was still possible to feel the oil in the surface. The film using φ = 0.10 also showed a satisfactory malleability and appearance compared to the φ = 0.15 film, a less oil quantity on its surface.

Considering the slight oil excess, the composition of the film was quantified to verify the oil amount and determine forms to avoid this problem. **Table 12** shows each film composition.

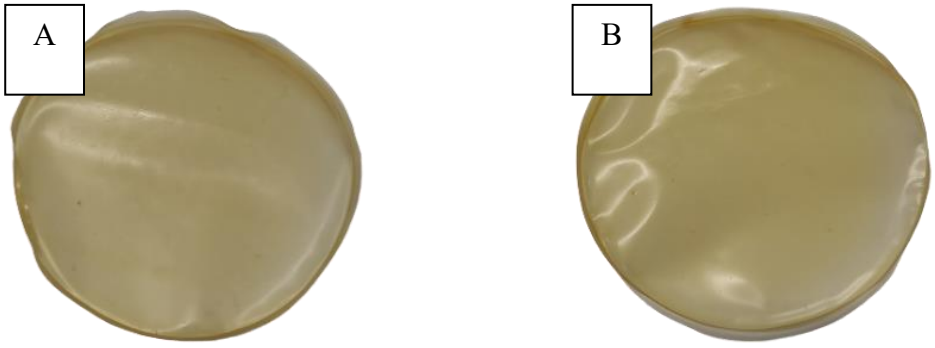

Figure 29 - Films (A) F_4.0%_r0.15_10/90_20% and (B) F_4.0%_r0.10_10/90_20%

Table 12 - Film mass composition.

Film	Films mass composition (%)		
	Oil	Ch/GA	GLY
F_4.0%_r0.10_10/90_20%	14.80	64.00	21.21
F_4.0%_r0.15_10/90_20%	20.49	58.83	20.68

Analyzing the results in **Table 12** it was possible to determine that the oil percentage into the film composition should be less than 14.80%. To this purpose, the casting

mixture was modified to by using an emulsion/plasticizer proportion of 05/95. Therefore, two new film formulations were prepared based on the emulsions with φ = 0.15 and φ = 0.10. **Figure 30** shows the formed films.

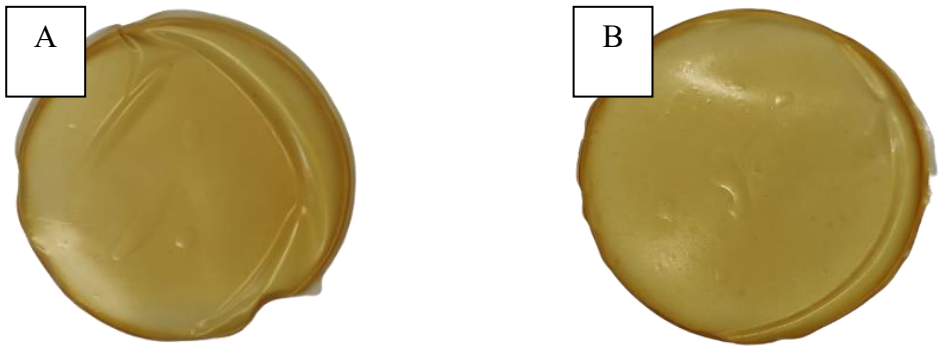

Figure 30 - Films formed: (A) Film F_4.0%_r0.15_05/95_20% by emulsion E_4.0%_r0.15_t_0 (B) Film F_4.0%_r0.10_05/95_20% by emulsion E_4.0%_r0.10_t_0.

From **Figure 30** it was possible to see a yellowish coloration for the formed films. This is due to the increase of the Ch/GA amount in the presence of GLY. Also, important to note that using this formulation, both films did not show the presence of free oil when touched. The formulation described here contained enough oil to be incorporated with the emulsion. Although both films showed similar results, the formulation using φ = 0.10 (F_4.0%_r0.10_05/95_20%) was selected, because of its texture, malleability, and appearance. As a reference, **Table 13** presents the composition obtained for each film.

Table 13 - Films composition using 4.0% (w/v) of the Ch/GA dispersion at a proportion 05/95 (emulsion/plasticizers).

Film	**Film composition (%)**		
	Oil	**Ch/GA**	**GLY**
F_4.0%_r0.10_05/95_20%	8.24	71.76	20.00
F_4.0%_r0.10_05/95_20%	11.76	68.16	20.09

Therefore, based on the formulation corresponding to the emulsion using φ = 0.10 and 4.0% (w/v) Ch/GA, and the film mixture formed by 5.00% of emulsion and 95.00% of Ch/GA dispersion-GLY, with GLY at 20%, it was possible to proceed to the next steps.

5.2.5. Incorporation of hydrophobic compounds in the Pickering emulsions

Initially, curcumin was used to verify the film capacity to incorporate the hydrophobic components into the matrix, then replaced with the turmeric extract. For this purpose, based on the formulation obtained in section 5.2.4 (E_4.0%_r0.10), curcumin was incorporated in a proportion of 0.5% relative to the oil mass. Since it is a hydrophobic component, its solubility is directly linked to the oily phase of the emulsion.

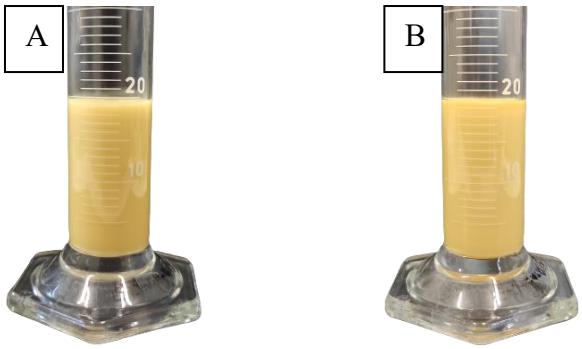

Figure 31 – Emulsion prepared using φ = 0.10, 4.0% (w/v) Ch/GA and 0.5% of curcumin. Emulsion (A) E_4.0%_r0.10_0.5%cur_t_0 and (B) E_4.0%_r0.10_0.5%cur_t_7.

Figure 31 shows the produced emulsion visual aspect over time. The emulsion showed a yellowish color on the production day, and seven days after. This coloration of the emulsion was derived from curcumin. The emulsion did not show apparent signs of instability.

The optical microcopy analysis of the emulsions is shown in **Figure 32**. From the microscopy, it was possible to observe droplets with spherical shapes, and apparent wide distribution of sizes. Also, it was discerned some curcumin crystals that can be attributed to the insufficient time for dissolution in the oil through bath sonication. The determined ADS values indicated a lower variability between the samples, including when compared to the previous formulations (E_4.0%_r0.10). The obtained values were 3.73 ± 0.81 μm at the t_0 and 3.82 ± 1.25 μm at the t_7.

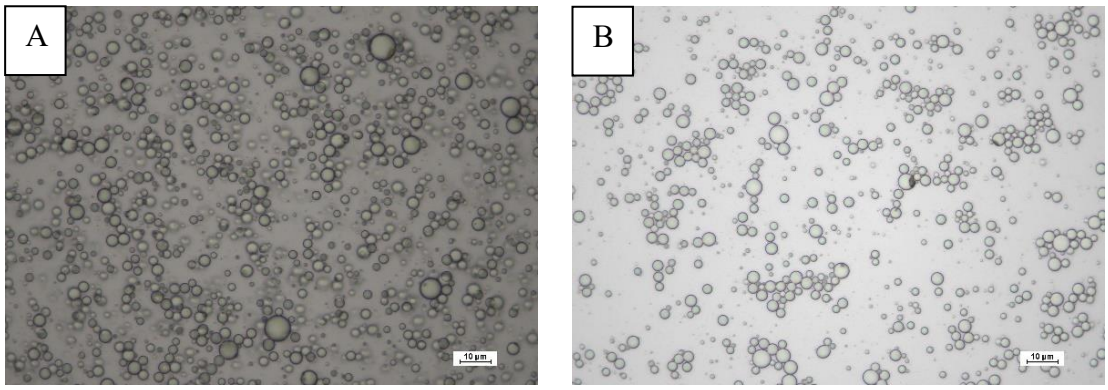

Figure 32 - Microscopy with 400x magnifications of emulsions (A) E_4.0%_r0.10_0.5%cur_t_0 and (B) E_4.0%_r0.10_0.5%cur_t_7.

The film prepared from this emulsion is shown in **Figure 33**. It has an orange hue color and a uniform thickness. Also, an increase in the stiffness was observed.

After the film production and incorporation of curcumin, used as a model sample, a new emulsion was tested using TE, the focus of this work. So, based on the emulsion E_4.0%_r0.10_0.5%cur, the emulsion containing turmeric extract and the corresponding functional film were prepared.

Figure 33 – The film formed using 5% of emulsion (φ = 0.10) and 95% Ch/GA dispersion (4.0% w/v) plus GLY (20% in relation to the film mass) – F_4.0%_r0.10_05/95_20%_0.5%cur.

Figure 34 shows the visual aspect of the emulsion at t_0 and t_7. The prepared emulsion was yellowish, similar to the one obtained with curcumin. A CI of zero was observed, indicative of a stable emulsion.

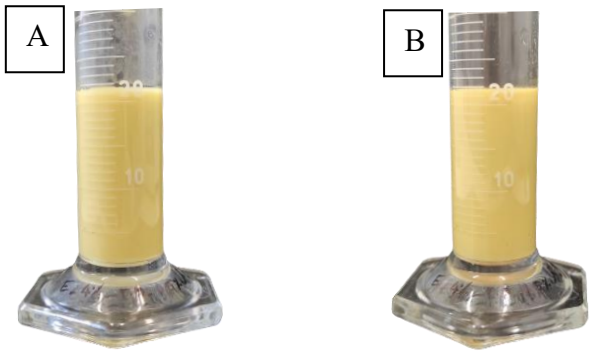

Figure 34 - Emulsion prepared using TE: (A) E_4.0%_r0.10_0.5%TE_t_0 and (B) E_4.0%_r0.10_0.5%TE_t_7.

Observing the results of the optical microscopy (**Figure 35**) it is possible to see droplets with a totally spherical shape morphology and a low ADS compared to the other systems. The emulsion at t_0 showed an ADS of 2.88 ± 0.70 μm and at t_7 3.05 ± 0.78 μm. These values showed a slight similarity with the formulation using curcumin, which is expected since this extract has a high curcumin content in its composition (Braga, et al., 2003).

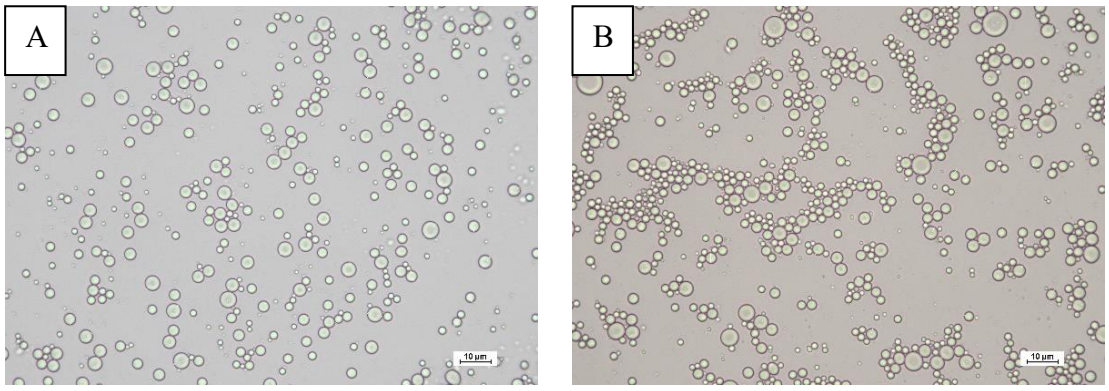

Figure 35 - Microscopy with 400x magnifications of the emulsions prepared using TE. (A) E_4.0%_r0.10_0.5%TE_t0 and (B) E_4.0%_r0.10_0.5%TE_t7.

The film, shown in **Figure 36**, presented a coloration similar to the one produced with curcumin and a higher homogeneity. These statements can evidence a better compatibility of TE in the system, compared with curcumin, since in the E_4.0%_r0.10_0.5%TE emulsion, no crystals were observed by OM, differently of the E_4.0%_r0.10_0.5%cur emulsion.

Figure 36 – The film formed using TE containing emulsion.

The composition of the film was also verified, and the obtained values are shown in **Table 14**. Analyzing the data in **Table 14** it was possible to observe that the oil amount was below 8.24%, corresponding to the most promising formulation for film production.

Table 14 – Composition of the film using TE containing emulsion.

Compound	Amount (%)
Oil	8.19%
Ch/GA	71.58%
Turmeric extract	0.04%
GLY	20.19%

5.3. CHARACTERIZATION OF THE MOST PROMISING PICKERING EMULSIONS

The most promising emulsion, i.e., the one containing TE with the formulation φ = 0.10 and a Ch/GA dispersion of 4.0% (w/v) was characterized. The base emulsion (i.e., the emulsion with no added TE using the same formulation) was also produced for comparison purposes.

5.3.1. CI and colorimetric evaluation

CI and the color were analyzed to compare the impact caused by using the extract. **Figure 37** shows both emulsions at t_0 and t_7. As explained in the previous sections, both emulsions gave rise to stable systems without serum layer formation (CI after a seven-day period was zero).

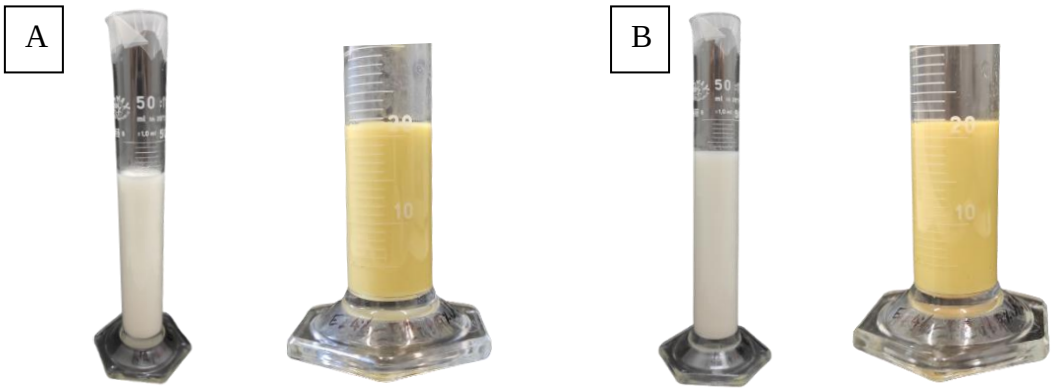

Figure 37 – Aspect of the base formulation (white) and emulsion added with TE (yellow) at (A) t_0 and (B) t_7.

The color of the emulsions was measured at t_0 and t_7. The CIELAB system to quantify the color was used. Observing the data in **Table 15**, it was possible to visualize a greater intensity in the b* index in the positive direction for the emulsion containing TE, thus justifying the yellow color accentuation of the emulsion. Also, it was observed a slight difference with the time, possible due to external environmental aspects at the time of measurement.

Table 15 - Emulsions coloration by L*a*b* scale.

Sample	Time	L*	a*	b*	RGB Color
Emulsion with 0.5% of turmeric extract	t0	71.81 ± 0.05	-2.00 ± 0.07	40.46 ± 0.06	
	t7	71.86 ± 0.14	-1.27 ± 0.11	40.50 ± 0.19	

Sample	Time	L*	a*	b*	RGB Color
Emulsion base	t0	81.83 ± 0.07	-1.32 ± 0.01	2.77 ± 0.02	
	t7	81.19 ± 0.32	-1.12 ± 0.02	2.52 ± 0.15	

5.3.2. Morphology

The optical microscope was utilized to quantify the samples' ADS and droplet size distribution (DS). Comparing the two emulsions, the same spherical shape was observed. The comparison of the systems can be seen in **Figure 38**.

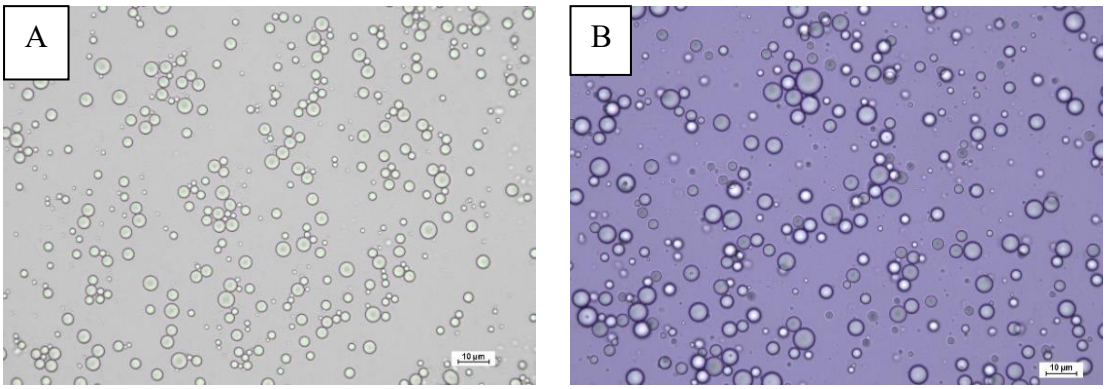

Figure 38 - Optical microscopy with 400x magnifications from (A) emulsion with TE and (B) emulsion base.

From the optical microscopy images, it was possible to build histograms that help to visualize how the emulsion droplet size is distributed. **Figure 39** represents the histograms obtained for the base emulsion at the two analyzed times. It was observed that more than 50% of the sample is within the size interval of 3 to 5 μm. Considering the forces involved in the destabilization process, it is possible to see the tendency to displace the DS to higher sizes. For this sample, the ADS at t_0 was 3.56 ± 1.36 μm and 4.94 ± 1.06 μm at t7.

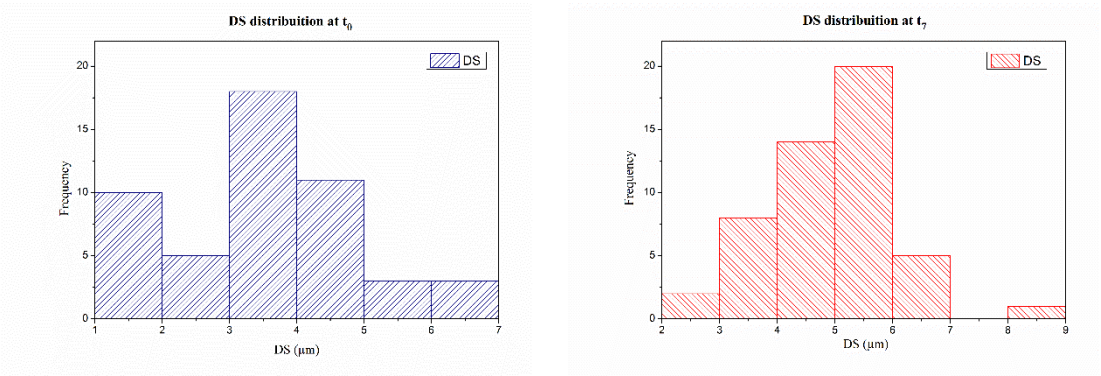

Figure 39 – Histogram of base emulsion DS distribution at t_0 and t_7.

Figure 40 shows the histograms of the TE-containing emulsion. This emulsion showed a narrower distribution than the base emulsion, ranging between 2.5 and 3.5 µm. It is possible to state that the extract affected the droplet formation in the emulsion. Some bigger droplets were observed for seven days, possibly due to destabilization phenomena. For the emulsion with TE, the ADS obtained at t_0 was 2.88 ± 0.70 µm and at t7 was 3.05 ± 0.78 µm, values lower than those observed for the base emulsion, thus, indicating an influence of the presence of the extract on the size of the particles, possibly due to an emulsifying capacity of the extract.

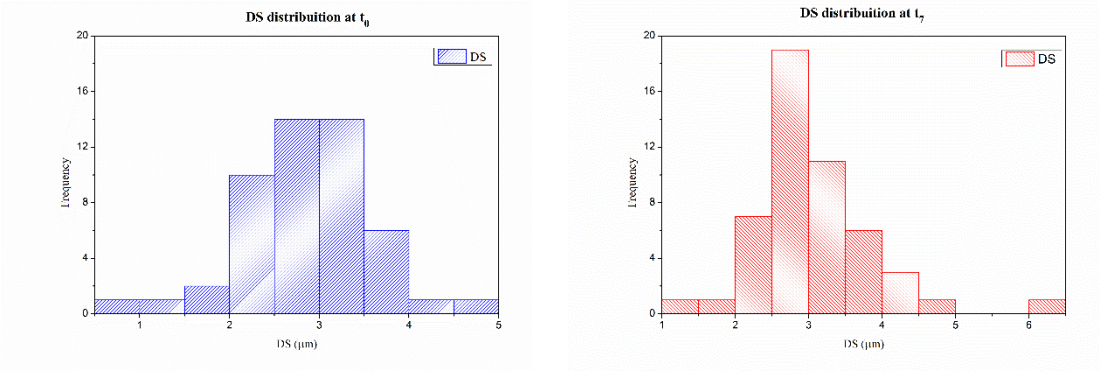

Figure 40 – Histograms of emulsion containing TE DS distribution at t0 and t7.

Therefore, these analyses corroborated the spherical shapes and size distributions that slightly displace towards higher sizes with time. Also, it was possible to visualize the effect of the extract in the emulsions acting in the decrease of the ADS and avoiding the

coalescence of the droplets and formation of large droplets for longer periods, if compared to the base emulsion.

5.4. CHARACTERIZATION OF THE MOST PROMISING FILMS

The base film and a film with TE were prepared and characterized. For both films, the color, transparency, and structural and functional characterization was analyzed by FTIR.

5.4.1. Colorimetric evaluation

The color of the films was determined using the CIELAB system. This analysis was performed after film total drying (t_0) and after seven days (t_7). The results obtained from these analyzes are shown in **Table 16**.

Table 16 – Films color by L*a*b* values.

Sample	time	L*	a*	b*	RGB Color
Film with TE	t_0	85.52 ± 0.10	-8.35 ± 0.04	58.49 ± 0.16	
	t_7	84.65 ± 0.29	-6.15 ± 0.22	55.84 ± 1.80	
Base film	t_0	87.40 ± 0.31	-7.34 ± 0.16	44.15 ± 0.62	
	t_7	86.41 ± 0.10	-6.45 ± 0.07	44.46 ± 0.34	

Observing the coloration of the films, it was possible to visualize the influence of the extract in the color. This influence concerned the greater intensity in the positive b*

index, the yellow color. Also, it was observed all values decreased over time. This decrease may be related to factors such as moisture absorption and the influence of light on the compounds. Nevertheless, this effect was of a slight dimension.

5.4.2. Films transparency

The visible spectroscopy technique (UV-vis) was used to analyze the films' transparency. The obtained spectra are represented in **Figure 41**.

Transparency is an optical property that quantifies the light barrier capacity, which means the material's characteristics to the light passage. Using Equation 3 and the data obtained from the UV-spectroscopy, it was possible to calculate the transparency. The values for each film are shown in the **Table 17**.

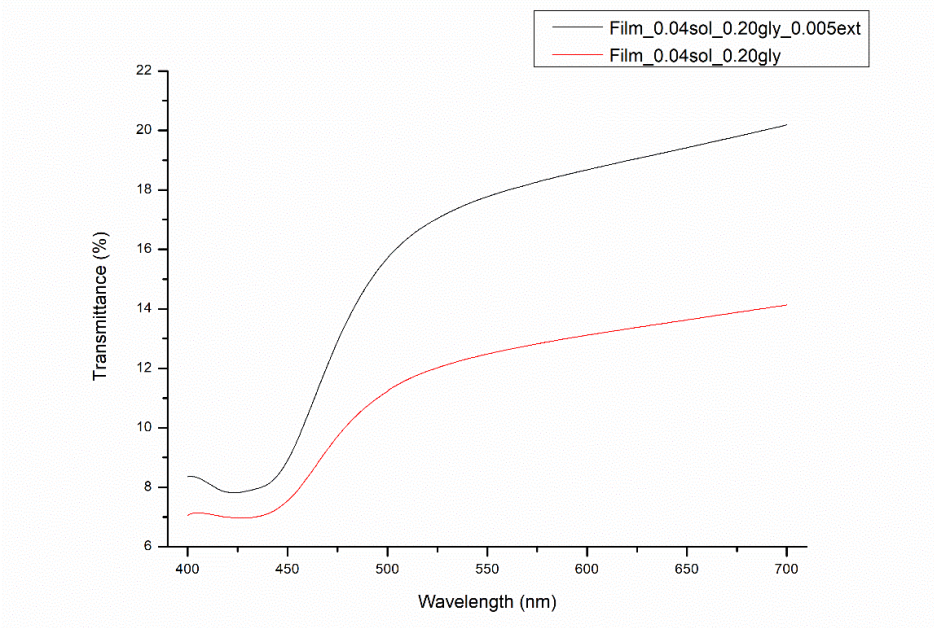

Figure 41 - UV-vis spectroscopy of the base film (Film_0.04sol_0.20gly) and film with TE (Film_0.04sol_0.20gly_0.005ext).

From the values reported in **Table 17**, it was possible to observe that the film with TE presented a higher transparency, even with the more intense coloration. This can be explained by using oil in its composition. Since Ch and GA are compounds with a high-

intensity signal, the presence of these components causes the intensity of this signal to be reduced, thus moving the molecules a little apart generating a greater free space (Xu, et al., 2019).

Table 17 - Films transparency determination.

Sample	L (mm)	T_{600} (%)	Transparency (%)
Film with TE	0.11 ± 0.01	18.67	11.66 ± 0.85
Base film	0.13 ± 0.01	13.16	8.34 ± 0.78

The transparency capacity relates to "transmit image-forming light" which in the package context is important to be as lower as possible (0 %); in this case, the film without TE presented better properties than the base film. Nonetheless, because the two films have responses close to zero, it becomes a positive feature for both formulations. (Zhao, et al., 2022).

5.4.3. FTIR analysis

The FTIR analysis of the materials present in the film, Ch, GA, SAO, turmeric extract, and the produced films were performed.

In the spectrum corresponding to Ch (**Figure 42**) it was possible to observe a large peak at 3370 cm^{-1} representing the hydroxyl groups. The sharp peak present at 2870 cm^{-1} indicates the alkanes presence. The presence of residual N-acetyl groups was confirmed by the bands at around 1651 cm^{-1} (C=O stretching of amide I) and 1320 cm^{-1} (C-N stretching of amide III), respectively. A band at 1580 cm^{-1} corresponds to the N-H bending of the primary amine. The bands around 1420 and 1372 cm^{-1} confirm the presence of CH_2 bending and CH_3 symmetrical deformations, respectively. The absorption band at 1134 cm^{-1} can be attributed to asymmetric stretching of the C-O-C bridge present in ethers. The bands corresponding to the C-O stretching can be observed around 1026 cm^{-1}. Finally, at 915 cm^{-1} it is possible to detect a CH bending out of the plane of the ring of monosaccharides. (Mohan, et al., 2020; Mittal, et al., 2021; Queiroz, et al., 2014)

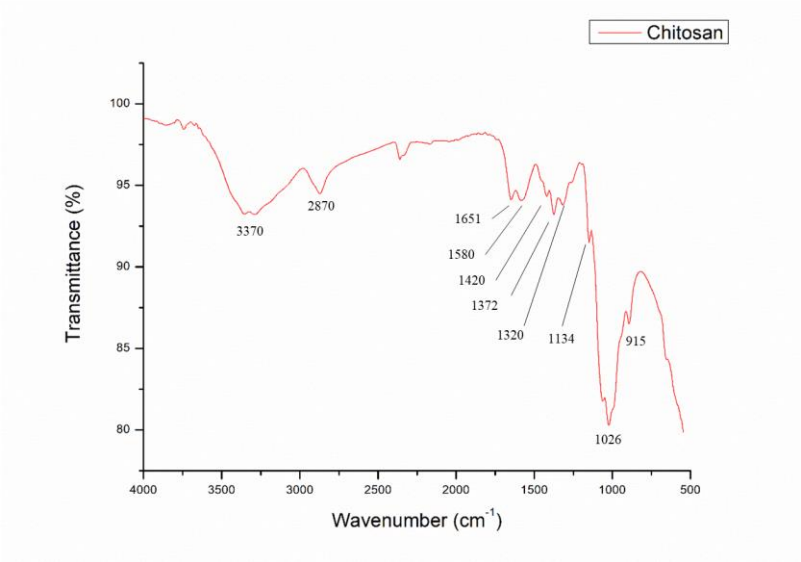

Figure 42 - FT-IR spectrum of Ch.

From the spectrum of GA (**Figure 43**) it was possible to observe at 3310 cm^{-1} the vibration ascribed to hydroxyl groups. Also, it was possible to visualize the C-H stretching corresponding to the peak at 2924 cm^{-1}. The peak at 1605 cm^{-1} can be assigned to the presence of C=O bonds. The 1420 cm^{-1} and 1018 cm^{-1} peaks are related to the presence of C-O groups (Xu, et al., 2019).

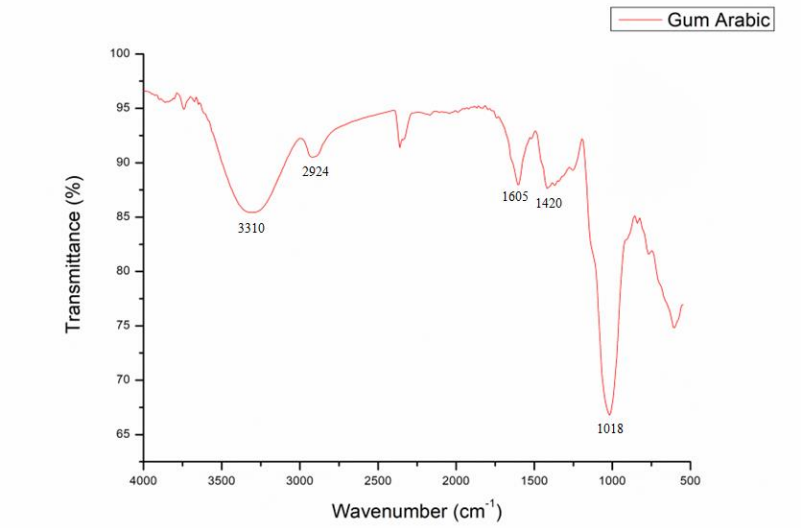

Figure 43 - FT-IR spectrum of GA.

In the SAO spectrum (**Figure 44**), it was possible to observe a band at 3007 cm^{-1} corresponding to the stretching of C-C bonds. At 2922 and 2853 cm^{-1} bands of symmetric and asymmetric C-H bond vibrations, respectively, are observed. The characteristic band of esters, C=O stretching vibration, is identified at 1742 cm^{-1}. Finally, at 1161 cm^{-1} it is possible to visualize a sharp peak, characteristic of C-O vibrations, accompanied by O-CH_2 bonds at 1096 cm^{-1}. (Hernández & Zacconi, 2009)

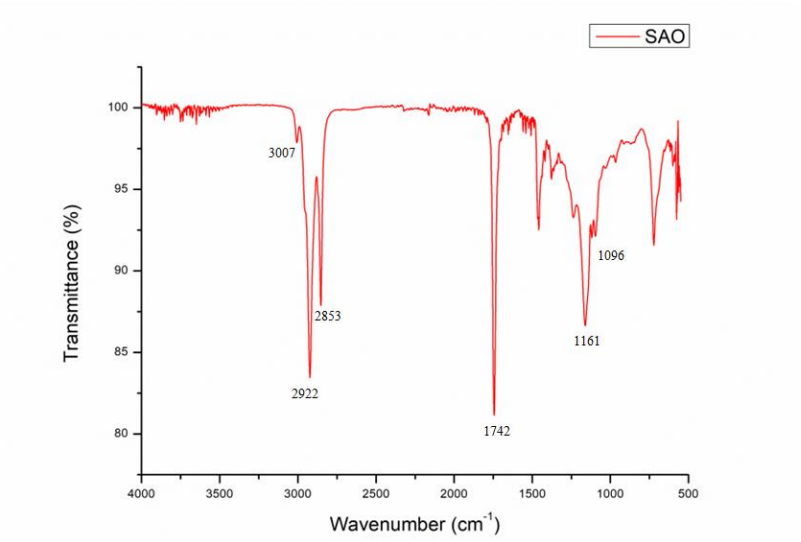

Figure 44 - FT-IR spectrum of SAO.

Figure 45 shows the spectrum corresponding to the TE utilized in film production. By the spectrum, it is possible to observe the presence of aromatic rings characterized by the bands at 1582, 1512, and 1434 cm^{-1}, concerning the bands of C=C bonds in aryl groups. Complementing, it is also possible to visualize the overlapping bands corresponding to =C-H aryl stretching vibrations at 3017 cm^{-1} and the C-H alkyl stretching vibrations at 2924 cm^{-1}. The medium-intensity broad-band at 3271 cm^{-1} indicates the presence of hydroxyl groups. The band present at 2361 cm^{-1} may indicate the presence of groups with triple bonds, which may be nitriles or carbons linked to other carbons. At 1674 cm^{-1} it can be observed the characteristic peak of C=C bonds. Finally, it is also possible to observe characteristic peaks of aromatic rings in the region between 750 and 1000 cm^{-1}. (Ismail, et al., 2014; Khamis, et al., 2019)

Finally, based on the previously analyzed spectra, the base film and the film added with TE were analyzed to identify possible interactions with adding the extract. **Figure 46** shows the spectra comparison.

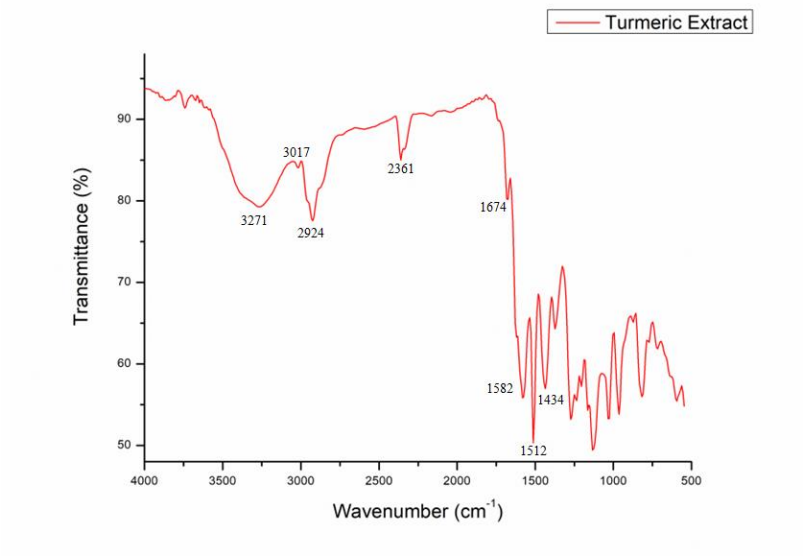

Figure 45 - FT-IR spectrum of TE.

In **Figure 46**, for both films it was possible to visualize the -OH stretching, present at 3225 cm^{-1}. Then, it is possible to observe in 2924 and 2870 cm^{-1} a merge between the -CH stretching vibration present in the Ch and GA spectra (2870 cm^{-1} in **Figure 42** for Ch and 2924 cm^{-1} in **Figure 43** for GA). Also, it is possible to observe the merge of the peaks 1651 cm^{-1} and 1580 cm^{-1} (representing C=O stretching of amide I and N-H bending of the primary amine, respectively) from Ch spectrum (**Figure 42**), and 1605 cm^{-1} peak from carboxyl group from GA (**Figure 43**) forming the peaks visualized at 1628 and 1551 cm^{-1}. At 1405 cm^{-1}, a peak of medium intensity is displayed, corresponding to the C=O stretching vibration. Finally, the 1026 cm^{-1} sharp peak corresponds to C-O stretching vibration.

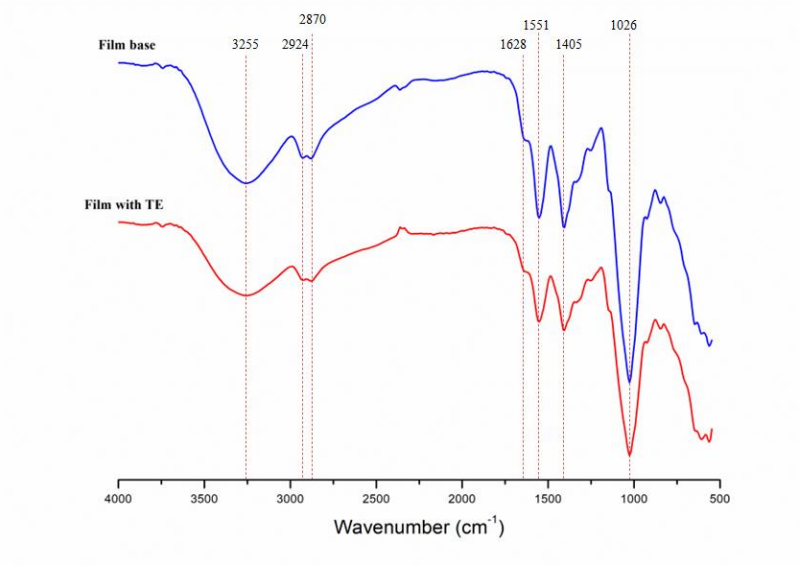

Figure 46 - FT-IR spectra of the base film and the film containing the TE

The peaks corresponding to TE and SAO were not observed, being the most discernible peaks related to the Ch and GA spectra. This result indicated that the TE could be encapsulated in the emulsion. Moreover, the small amount of the extract could make it difficult to identify it in the film spectrum.

6. CONCLUSIONS AND FUTURE WORKS

The Pickering emulsions technique, known as emulsions stabilized by solid particles, has increasingly gained space since they avoid using surfactants, or stabilizing agents. In addition to maintaining emulsion stability, it can provide different characteristics to emulsions. Based on this idea, Pickering emulsions were used as encapsulating agents for TE, the active component explored in this work, to functionalize films.

Under this context, the present work was conducted to produce and optimize a stable emulsified system of Pickering emulsions; produce and optimize films of hydrophilic nature added with hydrophobic components. The analysis and characterization of the produced emulsions and films were conducted.

TE was incorporated as an active hydrophobic component, which was successfully incorporated in a hydrophilic polymeric matrix using the Pickering emulsion technique. The created system comprised SAO, and Ch/GA particles as the dispersed phase and stabilizers, respectively. Ch/GA dispersions also formed the polymeric matrix to produce the film by the casting method, as such or added with the TE-loaded Pickering emulsion. This strategy enabled creating a film of hydrophilic origin functionalized with a hydrophobic compound (TE).

The production of emulsions and films and the effects generated in these systems due to the variation of some formulation parameters, such as solid particle concentration, and oil ratio, among others, were analyzed. During the development, several challenges were faced based on systems with few references available, thus becoming an innovative work in relation to the manufacture and application of these strategies to produce the films.

The results indicated the feasibility of implementing Pickering emulsions for producing hydrophilic matrix films functionalized with hydrophobic components. Through the work carried out, it was possible to observe and understand the behavior of the systems produced under different conditions. Among them, the effect of the concentration of solid particles, the oil ratio in the systems, the used plasticizers, and the types of hydrophobic components were verified.

The optimized system comprised an emulsion composition of $\varphi = 0.10$, using a Ch/GA dispersion at 4.0% (w/v) concentration and 0.5% TE (oil phase-basis). For the

film an emulsion/aqueous dispersion volume ratio of 5/95 with GLY at 20% of total film mass.

According to the conducted characterization, for the emulsions, a yellow coloring system with sufficient stability for the formation and drying of the film was observed when the TE was utilized. In addition, a system composed of spherical droplets with ADS of 3.76 ± 0.70 μm was observed. A yellowish material with a transparency of 18.67% was obtained for the films, demonstrating the influence of the plasticizer agent and the emulsion when compared to the base emulsion. It was also possible to the structural and functional characteristics of the films, observing the absence of evidence concerning the presence of the extract or oil, demonstrating the total incorporation of the emulsion or, alternatively, a low amount of extract to be detected.

For future work, it is recommended to evaluate films produced with different amounts of extract. Furthermore, it is also necessary to evaluate important aspects targeting the application of these films, e.g., food packaging materials. Among these parameters are: mechanical tests in order to validate and quantify the mechanical strength of the films; the water vapor permeability in order to understand and quantify the resistance of the films in terms of water absorption, thus avoiding the degradation of the materials protected by this film; the antioxidant and antimicrobial capabilities to verify the behavior of the film in order to protect food against oxidation and microbial agents; and shelf test to verify the useful life of the material.

REFERENCES

Ahmad, R. S. (2020). Biochemistry, safety, pharmacological activities, and clinical applications of turmeric: a mechanistic review. Evidence-based complementary and alternative medicine.

Aji, A. I., Praseptiangga, D., Rochima, E., Joni, I. M., & Panatarani, C. (2018, February). Optical transparency and mechanical properties of semi-refined iota carrageenan film reinforced with SiO2 as food packaging material. AIP conference proceedings (pp. Vol. 1927, No. 1, p. 030039). AIP Publishing LLC.

Albert, C., Beladjine, M., Tsapis, N., Fattal, E., Agnely, F., & Huang, N. (2019). Pickering emulsions: Preparation processes, key parameters governing their. Journal of Controlled Release, 309, 302-332.

Alencar, P. R., & Ribeiro, M. R. (2017). Desenvolvimento de um separador bifásico com aquecimento solar térmico para desestabilização de emulsões petróleo-água.

Alves, J. M., Olivo, P. M., Rodrigues, B. M., Ornaghi, M., Castilha, L. D., da Silva Junior, R. C., & dos Santos Pozza, M. S. (2019). Revestimento comestível a base de carragena e extrato de curcuma longa em ricotas. Brazilian Journal of Development, 5(8), 12656-12677.

Amalraj, A., Pius, A., Gopi, S., & Gopi, S. (2017). Biological activities of curcuminoids, other biomolecules from turmeric and their derivatives–A review. Journal of traditional and complementary medicine, 7(2), 205-233.

Atarian, M., Rajaei, A., Tabatabaei, M., Mohsenifar, A., & Bodaghi, H. (2019). Formulation of Pickering sunflower oil-in-water emulsion stabilized by chitosan-stearic acid nanogel and studying its oxidative stability. Carbohydrate polymers, 210, pp. 47-55.

Atkins, P., Paula, D. J., & Smith, D. (2017). Físico-Química - Fundamentos, 6ª edição. Rio de Janeiro: LTC.

Bansal, S., & Aggarwal, D. (2011). Color image segmentation using CIELab color space using ant colony optimization. International Journal of Computer Applications, 29(9), pp. 28-34.

Batista, J. A. (2004). Desenvolvimento, caracterização e aplicações de biofilmes a base de pectina, gelatina e ácidos graxos em bananas e sementes de brócolos. Campinas: Universidade Estadual de Campinas.

Bektas, E. I., Pekozer, G. G., Kök, F. N., & Kose, G. T. (2021). Evaluation of natural gum-based cryogels for soft tissue engineering. Carbohydrate Polymers, 118407.

Berton-Carabin, C. C., & Schroën, K. (2015). Pickering emulsions for food applications: background, trends, and challenges. Annual review of food science and technology, 263-297.

Braga, M. E., Leal, P. F., Carvalho, J. E., & Meireles, M. A. (2003). Comparison of yield, composition, and antioxidant activity of turmeric (Curcuma longa L.) extracts obtained using various techniques. Journal of agricultural and food chemistry, 51(22), pp. 6604-6611.

Briggs, N., Raman, A. K., Barret, L., Brown, C., Li, B., Leavitt, D., . . . Crossley, S. (2018). Stable pickering emulsions using multi-walled carbon nanotubes of varying. Colloids and Surfaces A: Physicochemical and Engineering Aspects, 227-235.

Bureau, L. (2014, 09 04). BLOG DA LE'ART. Retrieved from Blog Da Le'Art: https://blogdaleart.wordpress.com/2014/09/04/lab-color-o-espaco-de-cor/

Cen, K., Yu, X., Gao, C., Feng, X., & Tang, X. (2021). Effects of different vegetable oils and ultrasonicated quinoa protein nanoparticles on the rheological properties of Pickering emulsion and freeze-thaw stability of emulsion gels. Journal of Cereal Science, 102, 103350.

Chang, A. K., Frias Jr, R. R., Alvarez, L. V., Bigol, U. G., & Guzman, J. P. (2019). Comparative antibacterial activity of commercial chitosan and chitosan extracted from Auricularia sp. Biocatalysis and agricultural biotechnology, 17, pp. 189-195.

Chen, L., Ao, F., Ge, X., & Shen, W. (2020). Food-grade Pickering emulsions: Preparation, stabilization and applications. Molecules, 25(14), 3202.

da Silva Filho, C. R., Souza, A. G., Conceição, M. M., Silva, T. G., Silva, T., & Ribeiro, A. P. (2009). Avaliação da bioatividade dos extratos de cúrcuma (Curcuma longa L., Zingiberaceae) em Artemia salina e Biomphalaria glabrata. Revista Brasileira de Farmacognosia, 19, 919-923.

Daoub, R. M., Elmubarak, A. H., Misran, M., Hassan, E. A., & Osman, M. E. (2018). Characterization and functional properties of some natural Acacia gums. Journal of the Saudi Society of Agricultural Sciences, 241-249.

de Campos, S. S., de Oliveira, A., Moreira, T. F., da Silva, T. B., da Silva, M. V., Pinto, J. A., & Leimann, F. V. (2019). TPCS/PBAT blown extruded films added with curcumin as a technological approach for active packaging materials. Food Packaging and Shelf Life, 22, 100424.

De Carli, C., Aylanc, V., Mouffok, K. M., Santamaria-Echart, A., Barreiro, F., Tomás, A., . . . Falcão, S. I. (2022). Production of chitosan-based biodegradable active films using bio-waste enriched with polyphenol propolis extract envisaging food packaging applications. International Journal of Biological Macromolecules, 213, pp. 486-497.

Dror, Y., Cohen, Y., & Yerushalmi-Rozen, R. (2006). Structure of gum arabic in aqueous solution. Journal of Polymer Science Part B: Polymer Physics, 3265-3271.

Eugster, S. A. (2014, March 22). File:Curcuma longa roots.jpg. Retrieved from Wikipedia: https://en.wikipedia.org/wiki/File:Curcuma_longa_roots.jpg

Farias, M. G. (2016). Elaboração e caracterização de filmes de amido e polpa de acerola por casting, extrusão termoplástica e termoprensagem. Universidade Federal Rural do Rio de Janeiro, Seropédica - RJ: Tese (Doutorado em Ciência e Tecnologia de Alimentos) - Departamento de Tecnologia de Alimentos.

Fasihnia, S. H., Peighambardoust, S. H., Peighambardoust, S. J., Oromiehie, A., Soltanzadeh, M., & Peressini, D. (2020). Migration analysis, antioxidant, and mechanical characterization of polypropylene-based active food packaging films loaded with BHA, BHT, and TBHQ. Journal of Food Science, 85(8), pp. 2317-2328.

Feng, X., Dai, H., Ma, L., Fu, Y., Yu, Y., Zhou, H., . . . Zhang, Y. (2020). Properties of Pickering emulsion stabilized by food-grade gelatin. Colloids and Surfaces B: Biointerfaces, 111294.

Fu, L., Ma, Q., Liao, K., An, J., Bai, J., & He, Y. (2022). Application of Pickering emulsion in oil drilling. Nanotechnology Reviews, 11(1), 26-39.

Fujisawa, S., Togawa, E., & Kuroda, K. (2017). Nanocellulose-stabilized Pickering emulsions and their applications. Science and Technology of advanced MaTerialS, 959-971.

Ghirro, L. C. (2019). Desenvolvimento de emulsões Pickering para aplicação alimentar (Master dissertation). Bragança, Portugal: Instituto Politecnico de Braganca.

Gramatges, A. P. (2018). Nanopartículas de sílica funcionalizadas com grupos amônio e polímeros aniônicos para estabilização de emulsões Pickering contendo repelente de insetos. Doctoral dissertation, PUC-Rio.

Han, J., Chen, F., Gao, C., Zhang, Y., & Tang, X. (2020). Environmental stability and curcumin release properties of Pickering emulsion stabilized by chitosan/gum arabic nanoparticles. International journal of biological macromolecules, 157, 202-211.

Hay, E., Lucariello, A., Contieri, M., Esposito, T., De Luca, A., Guerra, G., & Perna, A. (2019). Therapeutic effects of turmeric in several diseases: An overview. Chemico-biological interactions, 310, 108729.

Hayati, I. N., Man, Y. B., Tan, C. P., & Aini, I. N. (2005). Monitoring peroxide value in oxidized emulsions by Fourier transform infrared spectroscopy. European Journal of Lipid Science and Technology, 886-895.

Heinrich, M., Williamson, E. M., Gibbons, S., Barnes, J., & Prieto-Garcia, J. (2017). Fundamentals of pharmacognosy and phytotherapy E-BOOK. Elsevier Health Sciences.

Hernández, S. A., & Zacconi, F. (2009). Aceite de almendras dulces: Extracción, caracterización y aplicación. Quimica Nova, 32, pp. 1342-1345.

Hong, I. K., Kim, S. I., & Lee, S. B. (2018). Effects of HLB value on oil-in-water emulsions: Droplet size, rheological behavior, zeta-potential, and creaming index. Journal of industrial and engineering chemistry, 67, 123-131.

Ibrahim, N. I., Shahar, F. S., Sultan, M. T., Shah, A. U., Safri, S. N., & Mat Yazik, M. H. (2021). Overview of bioplastic introduction and its applications in product packaging. Coatings, 11(11), 1423.

Ismail, E. H., Sabry, D. Y., Mahdy, H., & Khalil, M. M. (2014). Synthesis and Characterization of some Ternary Metal Complexes of Curcumin with 1, 10-phenanthroline and their Anticancer Applications. Journal of Scientific Research, pp. 509-519.

Isobe, N., Sagawa, N., Ono, Y., Fujisawa, S., Kimura, S., Kinoshita, K., & Deguchi, S. (2020). Primary structure of gum arabic and its dynamics at oil/water interface. Carbohydrate polymers, 249, 116843.

Jaafar, N. S. (2019). Clinical effects of Arabic gum (Acacia): A mini review. Iraqi Journal of Pharmaceutical Sciences (IJPS), 9-16.

Jahandideh, A., Ashkani, M., & Moini, N. (2021). Biopolymers in textile industries. In Biopolymers and Their Industrial Applications. Elsevier.

Jha, P. (2020). Effect of plasticizer and antimicrobial agents on functional properties of bionanocomposite films based on corn starch-chitosan for food packaging applications. International journal of biological macromolecules, 160, pp. 571-582.

Jiménez-Saelices, C., Trongsatitkul, T., Lourdin, D., & Capron, I. (2020). Chitin Pickering emulsion for oil inclusion in composite films. Carbohydrate polymers, 242, 116366.

Junior, M. J., & Varanda, L. C. (1999). O mundo dos colóides. QUÍMICA E SOCIEDADE, 9-13.

Kaewsaneha, C., Tangboriboonrat, P., Polpanich, D., Eissa, M., & Elaissari, A. (2013). Preparation of Janus colloidal particles via Pickering emulsion: An overview. Colloids and Surfaces A: Physicochemical and Engineering Aspects, 35-42.

Kempin, M. V., & Drews, A. (2021). What Governs Pickering Emulsion Properties During Preparation via Batch Rotor-Stator Homogenizers? Chemie Ingenieur Technik, 93(1-2), 311-317.

Kempin, M. V., Kraume, M., & Drews, A. (2020). Pickering emulsion preparation using a batch rotor-stator mixer–Influence on rheology, drop size distribution and filtration behavior. Journal of colloid and interface science, 573, 135-149.

Khamis, A. A., Sharshar, A. H., Mahmoud, A. H., & Mohamed, T. M. (2019). The Inhibitory Effect of Curcumin on Ornithine Decarboxylase against Hepatic Carcinoma. Journal of Biosciences and Medicines, 7(05), p. 127.

Koroleva, M. Y., & Yurtov, E. V. (2021). Ostwald ripening in macro-and nanoemulsions. Russian Chemical Reviews, 293.

Kumar, N., Gaur, T., & Mandal, A. (2017). Characterization of SPN Pickering emulsions for application in enhanced oil recovery. Journal of Industrial and Engineering Chemistry, 304-315.

Lauro, G. J. (2000). Natural food colorants: science and technology. CRC press.

Lira, A. L., Vesoloski, J. F., Peruzzolo, M., Flôres, D. Z., Cansian, R. L., & Paroul, N. (2021). Atividades antioxidante, antimicrobiana e compostos fenólicos de extratos comercial e in natura de Curcuma longa. Revista Perspectiva, 107-114.

Liu, Y., Sun, Y., & Huang, G. (2018). Preparation and antioxidant activities of important traditional plant polysaccharides. International Journal of Biological Macromolecules, 780-786.

Low, L. E., Siva, S. P., Ho, Y. K., Chan, E. S., & Tey, B. T. (2020). Recent advances of characterization techniques for the formation, physical properties and stability of Pickering emulsion. Advances in colloid and interface science, 102-117.

Manikantan, H., & Squires, T. M. (2020). Surfactant dynamics: hidden variables controlling fluid flows. Journal of fluid mechanics, 892.

Manual, I. (2002). Chroma meter cr-400/410. Japan: Konica Minolta Optics Inc.

Mcclements, D. J. (2007). Critical Review of Techniques and Methodologies for Characterization of Emulsion Stability. Critical reviews in food science and nutrition, 47(7), 611-649.

McClements, D. J. (2012). Advances in fabrication of emulsions with enhanced functionality using structural design principles. Current Opinion in Colloid & Interface Science, 235-245.

McClements, D. J. (2015). Food Emulsions: Principles, Practices, and Technique. Boca Raton: CRC Press.

McClements, D. J., & Jafari, S. M. (2018). Improving emulsion formation, stability and performance using mixed emulsifiers: A review. Advances in colloid and interface science, 55-79.

Melle, S., Lask, M., & Fuller, G. G. (2005). Pickering emulsions with controllable stability. Langmuir, 2158-2162.

Mittal, A., Singh, A., Benjakul, S., Prodpran, T., Nilsuwan, K., Huda, N., & de la Caba, K. (2021). Composite films based on chitosan and epigallocatechin gallate grafted chitosan: Characterization, antioxidant and antimicrobial activities. Food hydrocolloids, 111, p. 106384.

Mohammadinejad, R., Kumar, A., Ranjbar-Mohammadi, M., Ashrafizadeh, M., Han, S. S., Khang, G., & Roveimiab, Z. (2020). Recent advances in natural gum-based biomaterials for tissue engineering and regenerative medicine: A review. Polymers, 176.

Mohan, K., Ganesan, A. R., Muralisankar, T., Jayakumar, R., Sathishkumar, P., Uthayakumar, V., . . . Revathi, N. (2020). Recent insights into the extraction, characterization, and bioactivities of chitin and chitosan from insects. Trends in food science & technology, 105, pp. 17-42.

Morin-Crini, N., Lichtfouse, E., Torri, G., & Crini, G. (2019). Fundamentals and applications of chitosan. In Sustainable Agriculture Reviews. Springer, Cham, 49-123.

Mwangi, W. W. (2016). Effects of environmental factors on the physical stability of pickering-emulsions stabilized by chitosan particles. Food Hydrocolloids, pp. 60, 543-550.

Niro, C. M., Medeiros, J. A., Freitas, J. A., & Azeredo, H. M. (2021). Advantages and challenges of Pickering emulsions applied to bio-based films: a mini-review. Journal of the Science of Food and Agriculture, 101(9), pp. 3535-3540.

Niro, C. M., Medeiros, J. A., Freitas, J. A., & Azeredo, H. M. (2021). Advantages and challenges of Pickering emulsions applied to bio-based films: a mini-review. Journal of the Science of Food and Agriculture, 101(9), 3535-3540.

Ortiz, D. G., Pochat-Bohatier, C., Cambedouzou, J., Bechelany, M., & Miele, P. (2020). Current trends in Pickering emulsions: Particle morphology and applications. Engineering, 468-482.

Pardo-Castaño, C., & Bolaños, G. (2019). Solubility of chitosan in aqueous acetic acid and pressurized carbon dioxide-water: Experimental equilibrium and solubilization kinetics. The Journal of Supercritical Fluids, 151, pp. 63-74.

Pickering, S. U. (1907). Cxcvi.—emulsions. Journal of the Chemical Society, Transactions, 2001-2021.

Queiroz, M. F., Teodosio Melo, K. R., Sabry, D. A., Sassaki, G. L., & Rocha, H. A. (2014). Does the use of chitosan contribute to oxalate kidney stone formation? Marine Drugs, 13(1), pp. 141-158.

Ramsden, W. (1904). Separation of solids in the surface-layers of solutions and 'suspensions'(observations on surface-membranes, bubbles, emulsions, and mechanical coagulation).—Preliminary account. Proceedings of the royal Society of London, 156-164.

Ren, Z., Chen, Z., Zhang, Y., Lin, X., & Li, B. (2020). Characteristics and rheological behavior of Pickering emulsions stabilized by tea water-insoluble protein nanoparticles via high-pressure homogenization. International journal of biological macromolecules, 151, 247-256.

Ren, Z., Li, X., Ma, F., Zhang, Y., Hu, W., Khan, M. Z., & Liu, X. (2022). Oil-in-water emulsions prepared using high-pressure homogenisation with Dioscorea opposita mucilage and food-grade polysaccharides: Guar gum, xanthan gum, and pectin. LWT, pp. 162, 113468.

Rinaudo, M. (2006). Chitin and chitosan: Properties and applications. Progress in polymer science, 603-632.

Risch, S. J. (1995). Encapsulation: overview of uses and techniques.

Rodrigues, M. G., Vieira, T. B., Oliveira, M. L., Ferreira, L. A., Oliveira, R. E., Sousa, R. B., & Sousa, P. S. (2020). Classificação, composição e superfícies dos coloides no. Scientia Naturalis, 443-454.

Roy, S., & Rhim, J. W. (2021). Fabrication of carboxymethyl cellulose/agar-based functional films hybridized with alizarin and grapefruit seed extract. ACS Applied Bio Materials, 4(5), 4470-4478.

Roy, S., & Rhim, J. W. (2021). Preparation of pectin/agar-based functional films integrated with zinc sulfide nano petals for active packaging applications. Colloids and Surfaces B: Biointerfaces, 207,, 111999.

Ruivo, J. S. (2012). Fitocosmética: aplicação de extratos vegetais em cosmética e dermatologia. (Doctoral dissertation, [sn]).

Sadashiva, C. T., Hussain, H. F., & Nanjundaiah, S. (2019). Evaluation of hepatoprotective, antioxidant and cytotoxic properties of aqueous extract of turmeric rhizome (Turmesac®). Journal of Medicinal Plants Research, 13(17), 423-430.

Sahariah, P., & Másson, M. (2017). Antimicrobial chitosan and chitosan derivatives: a review of the structure–activity relationship. Biomacromolecules, 3846-3868.

Salager, J. L. (2002). Surfactants types and uses. Mérida.

Sánchez-Machado, D. I., López-Cervantes, J., Correa-Murrieta, M. A., Sánchez-Duarte, R. G., Cruz-Flores, P., & de la Mora-López, G. S. (2019). Chitosan. In Nonvitamin and nonmineral nutritional supplements. Academic Press, 485-493.

Schramm, L. L. (2005). Emulsions, Foams, and Suspensions: Fundamentals and Applications. Weinheim: WILEY-VCH Verlag GmbH & Co.

Shariatinia, Z. (2019). Pharmaceutical applications of chitosan. Advances in colloid and interface science, 131-194.

Sharkawy, A., Barreiro, M. F., & Rodrigues, A. E. (2019). Preparation of chitosan/gum Arabic nanoparticles and their use as novel stabilizers in oil/water Pickering emulsions. Carbohydrate polymers, 115190.

Sharkawy, A., Barreiro, M. F., & Rodrigues, A. E. (2020). Chitosan-based Pickering emulsions and their applications: A review. Carbohydrate polymers, 250, 116885.

Shawn, D. J. (1975). Introdução à Química dos Colóides e de Superfícies. São Paulo: E. Blücher.

Silva, G. T. (2018). Estudo da coalescência de gotas de óleo em água. Rio de Janeiro: PUC-Rio.

Sun, H., Li, S., Chen, S., Wang, C., Liu, D., & Li, X. (2020). Antibacterial and antioxidant activities of sodium starch octenylsuccinate-based Pickering emulsion films incorporated with cinnamon essential oil. International Journal of Biological Macromolecules, 159, pp. 696-703.

Tadros, T. (2004). Application of rheology for assessment and prediction of the long-term physical stability of emulsions. Advances in colloid and interface science, 227-258.

Taghavi Fardood, S., Ramazani, A., & Woo Joo, S. (. (2018). Eco-friendly synthesis of magnesium oxide nanoparticles using arabic Gum. Journal of Applied Chemical Research, 8-15.

Teixeira, S. C., Silva, R. R., de Oliveira, T. V., Stringheta, P. C., Pinto, M. R., & Soares, N. D. (2021). Glycerol and triethyl citrate plasticizer effects on molecular, thermal, mechanical, and barrier properties of cellulose acetate films. Food Bioscience, 42, p. 101202.

Tharanathan, R. N. (2003). Biodegradable films and composite coatings: past, present and future. rends in food science & technology, 14(3), 71-78.

Thornfeldt, C. (2005). Cosmeceuticals containing herbs: fact, fiction, and future. Dermatologic Surgery, 31, 873-881.

Varanda, L. C. (1999). Estudo da forma e da distribuição de tamanho de partículas de alumina em dispersões coloidais relacionado a sedimentação gravitacional.

Verma, R. K., Kumari, P., Maurya, R. K., Kumar, V., Verma, R. B., & Singh, R. K. (2018). Medicinal properties of turmeric (Curcuma longa L.). Int. J. Chem. Stud, 6(4), 1354-1357.

Vollhardt, J. (2000). Natural extracts for baby care. Cosmetics and toiletries, 115(11), 63-73.

Wang, L. J., Hu, Y. Q., Yin, S. W., Yang, X. Q., Lai, F. R., & Wang, S. Q. (2015). Fabrication and characterization of antioxidant pickering emulsions stabilized by zein/chitosan complex particles (ZCPs). Journal of Agricultural and Food Chemistry, 63(9), pp. 2514-2524.

Xia, T., Xue, C., & Wei, Z. (2021). Physicochemical characteristics, applications and research trends of edible Pickering emulsion. Trends in Food Science & Technology, 1-15.

Xu, T., Gao, C., Feng, X., Yang, Y., Shen, X., & Tang, X. (2019). Structure, physical and antioxidant properties of chitosan-gum arabic edible films incorporated with cinnamon essential oil. International journal of biological macromolecules, 134, pp. 230-236.

Yang, H., Su, Z., Meng, X., Zhang, X., Kennedy, J. F., & Liu, B. (2020). Fabrication and characterization of Pickering emulsion stabilized by soy protein isolate-chitosan nanoparticles. Carbohydrate polymers, 116712.

Zamani, S. M. (2018). Formation of shelf stable Pickering high internal phase emulsions (HIPE) through the inclusion of whey protein microgels. Food & Function, pp. 9(2), 982-990.

Zhang, T., Xu, J., Zhang, Y., Wang, X., Lorenzo, J. M., & Zhong, J. (2020). Gelatins as emulsifiers for oil-in-water emulsions: Extraction, chemical composition, molecular structure, and molecular modification. Trends in Food Science & Technology, 113-131.

Zhao, J., Wang, Y., & Liu, C. (2022). Film Transparency and Opacity Measurements. Food Analytical Methods, 15(10), pp. 2840-2846.

Zhou, L., Zhang, J., Xing, L., & Zhang, W. (2021). Applications and effects of ultrasound assisted emulsification in the production of food emulsions: A review. Trends in Food Science & Technology, 493-512.

Zhu, F. (2019). Starch based Pickering emulsions: Fabrication, properties, and applications. Trends in Food Science & Technology, 129-137.

APPENDIX A

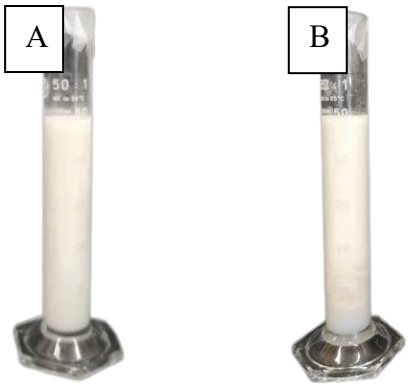

Figure A1 – Emulsions (A) E_5.0%_r0.30_t_0 and (B) E_5.0%_r0.30_t_7.

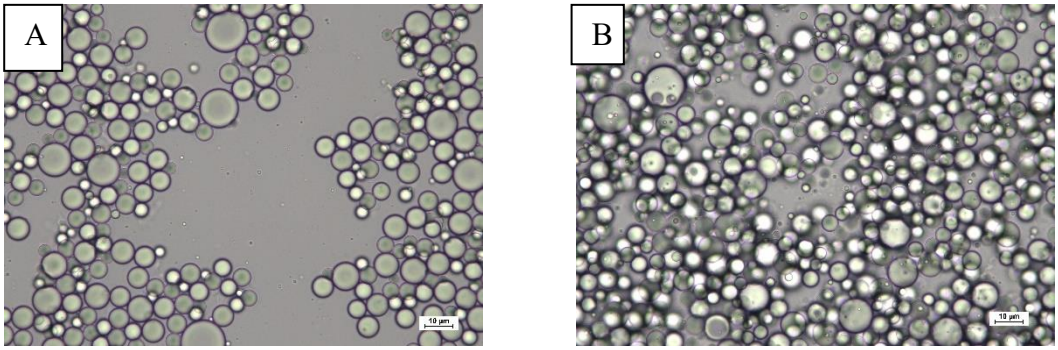

Figure A2 – OM with 400x magnifications of emulsions (A) E_5.0%_r0.30_t_0 and (B) E_5.0%_r0.30_t_7.

Figure A3 – Film F_5.0%_r0.30_10/90 formed by emulsions E_5.0%_r0.30_t_0.

APPENDIX B

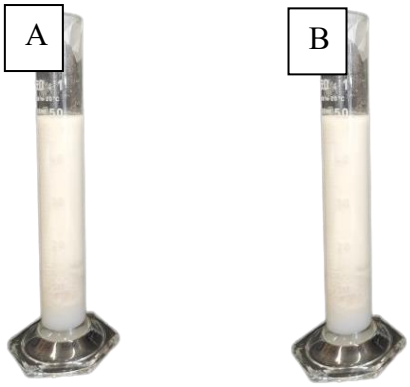

Figure B1 – Emulsions (A) E_4.0%_r0.20_t_0 and (B) E_4.0%_r0.20_t_7, using acetic acid 0.1N.

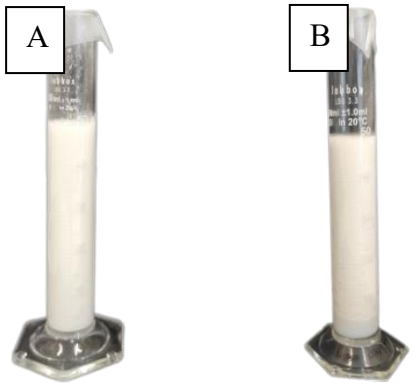

Figure B2 – Emulsions (A) E_5.0%_r0.20_t_0 and (B) E_5.0%_r0.20_t_7, using acetic acid 0.1N.

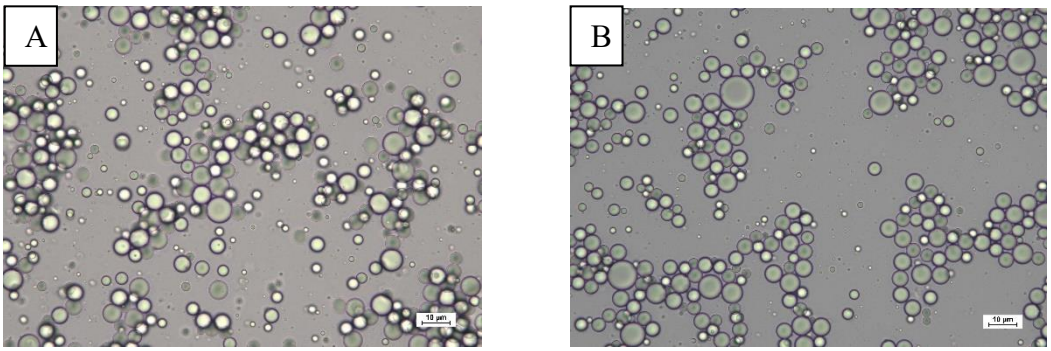

Figure B3 – OM with 400x magnifications of emulsions (A) E_4.0%_r0.20_t_0 and (B) E_4.0%_r0.20_t_7.

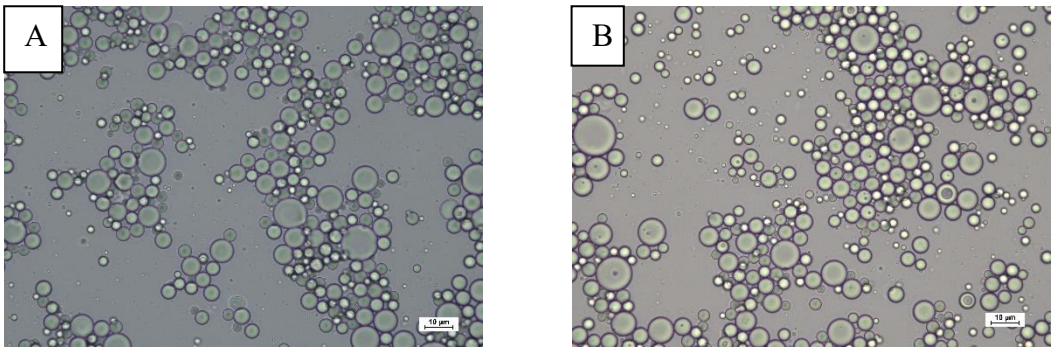

Figure B4 – OM with 400x magnifications of emulsions (A) E_5.0%_r0.20_t_0 and (B) E_5.0%_r0.20_t_7.

Figure B5 – Film F_4.0%_r0.20_10/90 formed by emulsions E_4.0%_r0.20_t_0.

Figure B6 – Film F_5.0%_r0.20_10/90 formed by emulsions E_5.0%_r0.20_t_0.

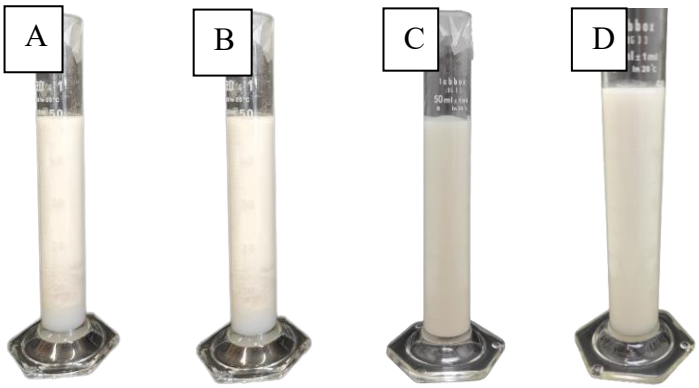

Figure B7 – Emulsion (A) E_4.0%_r0.20_t_0 and (B) E_4.0%_r0.20_t_7, using acetic acid 0.1N; (C) E_4.0%_r0.20_t_0 and (D) E_4.0%_r0.20_t_7 using acetic acid 0.3N.

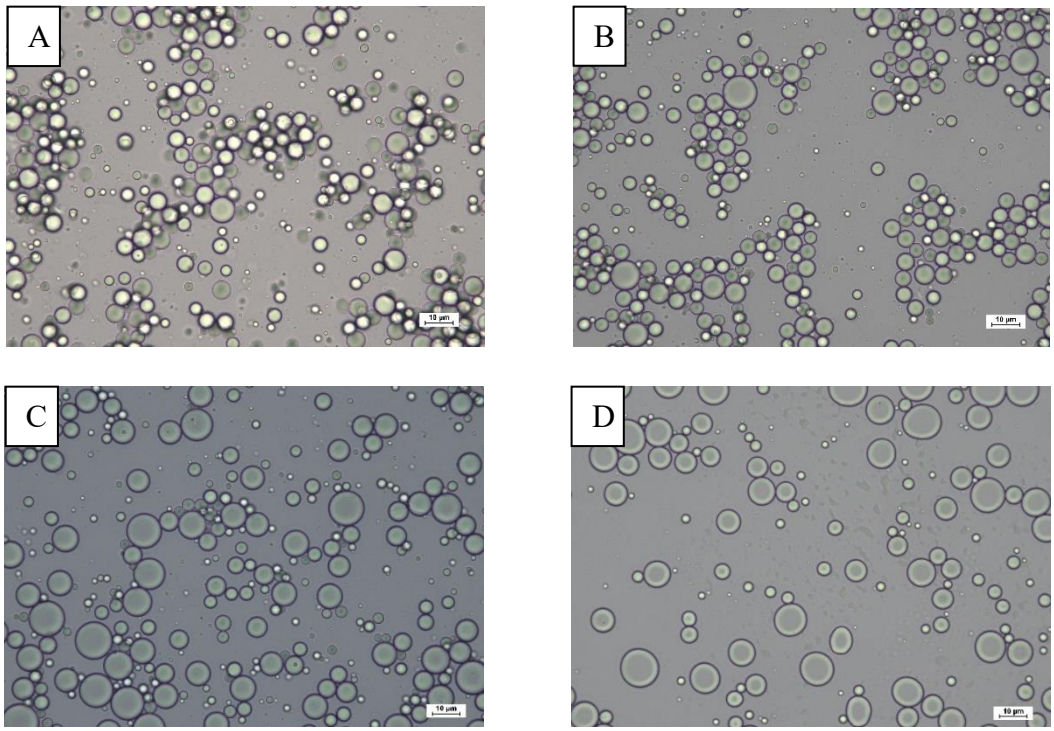

Figure B8 – OM with 400x magnifications of emulsion (A) E_4.0%_r0.20_t_0 and (B) E_4.0%_r0.20_t_7, using acetic acid 0.1N; (C) E_4.0%_r0.20_t_0 and (D) E_4.0%_r0.20_t_7 using acetic acid 0.3N.

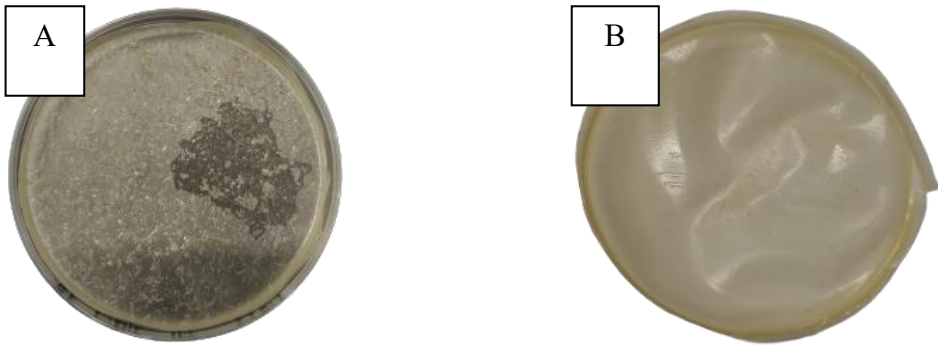

Figure B9 – Comparison between films type F_4.0%_r0.20_10/90 using (A) acetic acid 0.1N and (B) acetic acid 0.3N.

APPENDIX C

Figure C1 – Film F_4.0%_r0.20_10/90_25% produced by emulsion E_4.0%_r0.20_t_0.